

We are IntechOpen, the world's leading publisher of Open Access books Built by scientists, for scientists

4,800

Open access books available

122,000

International authors and editors

135M

Downloads

Our authors are among the

154

Countries delivered to

TOP 1%

most cited scientists

12.2%

Contributors from top 500 universities



WEB OF SCIENCE™

Selection of our books indexed in the Book Citation Index
in Web of Science™ Core Collection (BKCI)

Interested in publishing with us?
Contact book.department@intechopen.com

Numbers displayed above are based on latest data collected.
For more information visit www.intechopen.com



Heterogeneous Melting in Low-Dimensional Systems and Accompanying Surface Effects

Dmitry G. Gromov and Sergey A. Gavrilov
*Moscow Institute of Electronic Technology
Russia*

1. Introduction

It is well known that the smaller the size of low-dimensional objects the lower melting temperatures they have. This effect is described in its various manifestations in numerous both old enough and comparatively recent publications.

However, for quite objective reasons, the mechanisms of the observed phenomena in low-dimensional systems are still discussed, as it remains unclear whether these phenomena can be called melting or not.

The evolution of different material thin films during heating has been repeatedly studied. Heating is known to result in thin-film disintegration into droplets (or, in other terms, beads), if a film has been deposited on an inert surface. However, there exists no unified understanding of this phenomenon; hence, there is no generally accepted terminology. It should be noted that in various research this phenomenon goes under different terms, e.g. breaking up, rupture, reflow, agglomeration, disintegration, dewetting, decay or beading of a thin film, melting, surface premelting, surface-induced melting.

The aim of this chapter is to analyze the specific features of heterogeneous melting and to show, on the basis of experimental research, that heterogeneous melting mechanism starts to play an important role as the system size decreases and initiates a number of processes that are frequently encountered in micro- and nanotechnologies. It should be noted that the reason for different points of view on this phenomenon is hidden in the peculiarities of the melting process.

Classical equilibrium thermodynamics strictly determines the temperature of the phase transition solid-liquid and vice versa. According to it, it is the temperature at which one can observe the equality of the Gibbs potential of solid and liquid phases.

In accordance with equilibrium thermodynamics, at constant pressure in a one-component system phase transition occurs at a specific temperature and it should be accompanied by a sudden change in heat release or absorption, i.e. phase transition has no extension in time or hysteresis. It should be noted, that although interphase border is an integral part of any system where phase transition takes place, classical equilibrium thermodynamics does not pay any attention to the possible contribution of this border to phase transitions.

While observing the phenomenon researchers often see a paradox. The melting process, accompanied by heat absorption and not a spontaneous one, and therefore requiring more energy for the system, occurs at the reference temperature. This temperature is defined as equilibrium melting temperature, and the melting process here does not require

overheating. At the same time the crystallization process, which is accompanied by heat release and is spontaneous and therefore does not require more energy for the system, occurs at the temperature lower than the reference one, i.e. this process needs overcooling. Thus, phase transition is asymmetric.

The cause of this paradox becomes clear only after taking into account the contribution of interphase border to phase transition. Here we can distinguish two extreme cases: homogeneous and heterogeneous. In a homogeneous case, phase transition is the transition from a monophase state, in which there is no surface, to a two-phase state, in which phases are separated from each other by the interphase surface. So, a homogeneous case requires energy to create phase interface. Heterogeneous case occurs when two-phase state exists meaning that phase interface exists as well, i.e. there is no need for applying energy.

In the real material world, any system is finite or at least semi-infinite, i.e. regardless of its size somewhere it comes to an end with a surface. As a surface is the main defect of a three-dimensional crystal lattice, its vibration spectrum differs from the bulk spectrum. Vibration amplitude of atoms located on the surface is always higher than that in the bulk. It is an established fact that vibration amplitude of atoms located close to the surface is 40-100% higher than atoms in the bulk. Consequently the Debye temperature of a surface layer is approximately half the Debye temperature characteristic of the bulk phase. This means that the crystal surface can melt at a temperature of half the melting temperature of the bulk material.

That is why melting always begins from the surface, the melt front moves inward the crystal. Thus, the melting process is heterogeneous, it does not require energy to create interface surface of solid and liquid phases, and the material completely melts at the equilibrium melting temperature indicated in reference books.

For the same reason of higher amplitude of near-surface atomic vibrations, crystallization cannot start from the liquid-phase surface. Because of this, unlike the melting process, the crystallization process is homogeneous and needs overcooling of the system by dozens or even hundreds degrees relative to the equilibrium temperature of the phase transition.

At the same time, as a solid-phase surface is artificially introduced, the heterogeneous crystallization, which almost does not require any overcooling of the liquid phase, also easily proceeds. The example of such process can be crystal growth as in the case of pulling out single crystals from a melt. Here to fulfill the phase transition overheating or overcooling should be only a few degrees; there is practically no hysteresis and the process is close to equilibrium.

One should not forget that along with the process of phase transition – melting-crystallization, the process of solidification-dilution also takes place and this process is not phase transition. The essence of this process consists in changing viscosity (or fluidity) of liquid phase depending on temperature. Being independent, this process has a great influence on the process of crystallization. The greatest influence of this process can be observed in creating solid amorphous state when because of higher viscosity with lower temperature, crystalline phase cannot occur.

2. Heterogeneous melting in semi-infinite systems

As it is stated earlier equilibrium temperature of phase transition from solid to liquid state T_{∞} in an equilibrium thermodynamic system is the temperature when one can observe the equality of the Gibbs potential of solid and liquid phases (Fig. 1):

$$G_S = G_L \quad (1)$$

i.e.

$$H_S - T_\infty S_S = H_L - T_\infty S_L \tag{2}$$

From equation (2) the entropy change in transition from solid to liquid state, we have

$$\Delta S(T_\infty) = \frac{\Delta H(T_\infty)}{T_\infty} \tag{3}$$

where $\Delta H(T_\infty)$ is the change in the enthalpy of the system upon transition from a solid state to a liquid state at the corresponding temperature T_∞ .

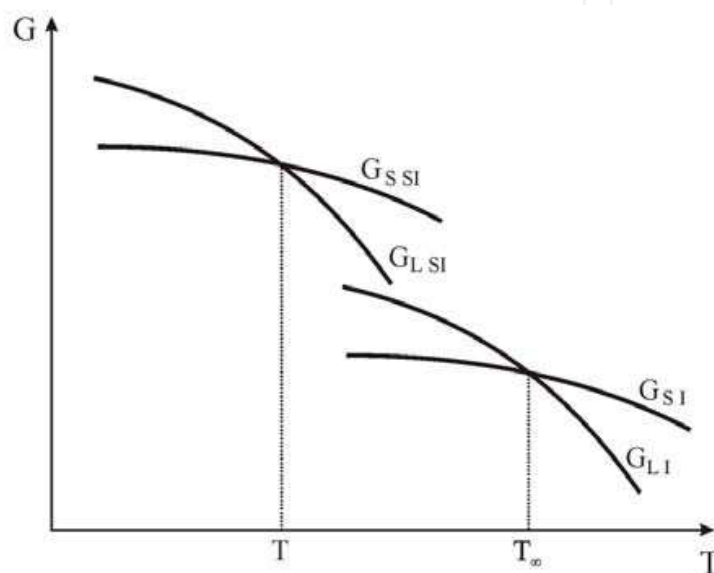


Fig. 1. The dependence of Gibbs energy from the temperature of solid and liquid phases in a single-component infinite (G_I) and semi-infinite (G_{SI}) system.

Equation (2) is correct for infinite systems where there is no contribution of energy of the surface to the total energy of the system. For the semi-infinite system having a limiting surface, under assumption that the volume remains unchanged after the phase transition, equality (2) transforms into the equation:

$$H_S - TS_S + \sigma_S \frac{A_S}{V} = H_L - TS_L + \sigma_L \frac{A_L}{V} \tag{4}$$

where T is temperature of the phase transition in semi-infinite system, σ is surface energy, A is surface area, V is volume. One should bear in mind that H and S must be on volume unit (J/m^3).

Additional components in equation (4) in comparison with equation (2) lead to the higher Gibbs potential and curve shift of free enthalpy changes of solid and liquid phases as in Fig.1. The result is that equilibrium point of phase shifts from T_∞ to lower temperatures T . From transposition of the components in equation (4) we see

$$T\Delta S(T) = \Delta H(T) + \frac{\sigma_L A_L - \sigma_S A_S}{V} \tag{5}$$

Entropy is a thermodynamic function defining the degree of an order in system. The degree of an order changes in transition from ordered crystalline state to disordered liquid state. This leads us to the fact that although entropy depends on the system temperature, the change of entropy in the transition from crystalline state to liquid state does not depend much on temperature at which it occurs, i.e.

$$\Delta S(T) \approx \Delta S(T_\infty) \quad (6)$$

To obtain the dependence between melting temperatures T_∞ in an infinite system and T in a semi-infinite system, we substitute (6) for (5) considering (3)

$$T = T_\infty \left(\frac{\Delta H(T)}{\Delta H(T_\infty)} + \frac{\sigma_L A_L - \sigma_S A_S}{V \Delta H(T_\infty)} \right) \quad (7)$$

Equation (7) depicts the change of melting temperature due to contribution of the surface under constant pressure.

However, there may be an assumption that melting heat does not depend on the temperature at which the phase transition occurs:

$$\Delta H(T) \approx \Delta H(T_\infty) \quad (8)$$

Taking into account that under phase transition the area surface does not change $A_L = A_S$, assumption (8) and that $V = Ah$, we obtain a well-known equation that describes the decreasing temperature of thin film depending on its thickness h

$$T = T_\infty \left(1 + \frac{\Delta \sigma}{\Delta H(T_\infty) h} \right) \quad (9)$$

where $\Delta \sigma$ is the change in surface energy as a result of transition from the crystalline state to the liquid state.

From equation (9) we can derive the expression for the approximate evaluation of the equilibrium thickness of a molten surface layer as a function of the temperature

$$h = \frac{T_\infty \Delta \sigma}{(T - T_\infty) \Delta H(T_\infty)} \quad (10)$$

We calculated the dependence of the thickness of the molten layer on temperature for lead using the following initial data. For the free upper surface of a lead film we take the energies of the lead surface adjacent to vacuum $\sigma_S = 0.56 \text{ J/m}^2$ and $\sigma_L = 0.44 \text{ J/m}^2$. We assume that the surface layer undergoing the melting process is initially a thin lead film laying on the lead surface. Our comparison of the calculated and experimental data show that the boundary energy between solid phases or liquid and solid phases is best represented by the arithmetic mean of the surface energies of the corresponding materials. Because of this, we use $\sigma_S = 0.56 \text{ J/m}^2$ also for the lead-lead solid phase boundary and $\sigma_L = 0.5 \text{ J/m}^2$ for the liquid lead-solid lead boundary. The melting heat of lead (per unit volume) was $\Delta H(T_\infty) = 2.7 \times 10^8 \text{ J/m}^3$. Fig. 2 illustrates the estimated dependency of the thickness of molten surface layer on the temperature of lead. The kind of dependency in Fig. 2 coincides with experimental curve, which is the result of the medium-energy ion dissipation method that allows us to determine the depth of unregulated layer on the surface. As it is shown in Fig. 2, the essence

of this phenomenon is that at temperatures much lower than the temperature of melting, an unregulated liquid layer appears on the surface of semi-infinite crystalline body. The thickness of the layer rises fluently at first, and then it rises very abruptly as the temperature rises, leading to complete melting at the equilibrium temperature T_{∞} . B.Pluis and his colleagues named this phenomenon "surface-induced melting". As we see it, this term reflects the essence of the phenomenon in the best way. Another term for this phenomenon is "heterogeneous melting".

Three distinctive areas can be distinguished in the phenomenon of heterogeneous melting (Fig. 2). Area III, which is situated higher than the equilibrium temperature of melting T_{∞} is the area where the crystalline phase is completely molten and the liquid phase alone exists. Area I and Area II both are characterized by coexistence of crystalline and liquid phases of the matter. However, in Area I, where the thickness of the molten layer is lesser than 20 nm, the quantity of the matter in liquid state does not correspond to physicochemical concept of "phase". In this area, the liquid layer can be regarded rather as an adsorption layer that lowers the surface energy of semi-infinite crystalline phase. In this case, the liquid layer and the semi-infinite crystalline phase are a single system. In Area II the liquid layer on the surface becomes a phase and can be regarded as an independent system that coexists in contact with another system, i.e., the crystalline phase. Properly, it is Area II that can be rightfully regarded as the area of the surface-induced melting process.

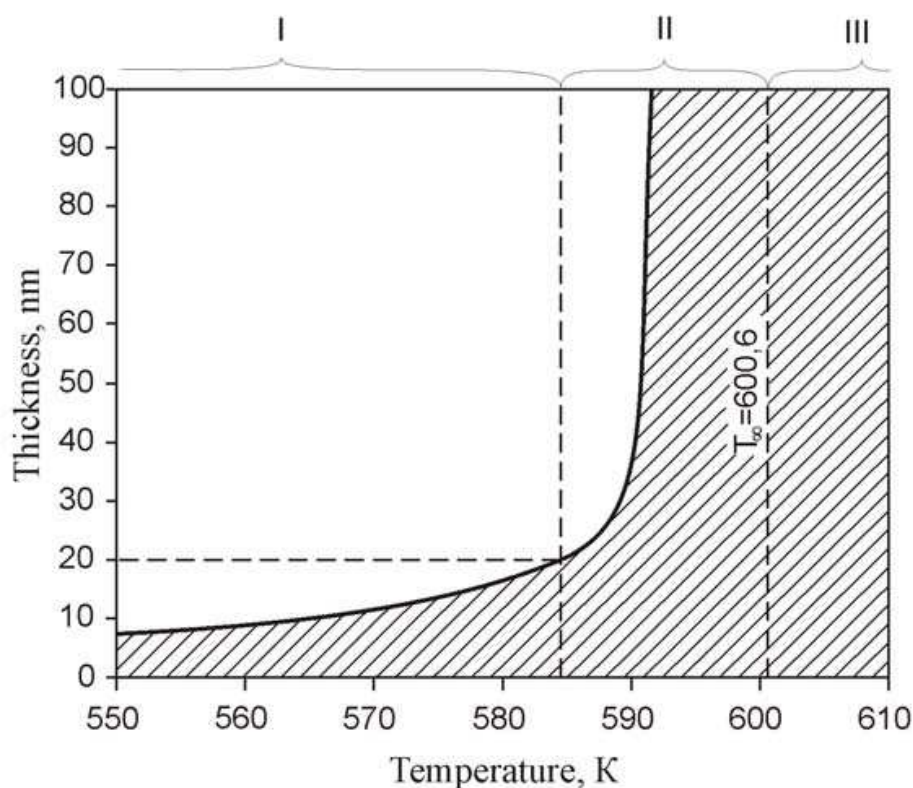


Fig. 2. Heterogeneous melting of lead: the estimated dependency of the thickness of the molten surface layer on temperature.

Thereby, the shape of the curve in Fig. 2 leads to two important conclusions:

- The existence of a surface in a semi-infinite system, and, as a consequence, the appearance of the phenomenon of melting which is caused by this surface, lead to the

fact that the complete melting of the semi-infinite phase occurs at the temperature of equilibrium phase conversion of an infinite system of the same kind of matter virtually in all cases. In other words, the absence of necessity to input energy to create a surface in a semi-infinite system always leads to heterogeneous melting, which requires no overheating comparative to equilibrium melting temperature of an infinite system;

- At the temperature that is lower than the reference temperature, on the surface of the solid phase there exists a layer of liquid phase of definite thickness, which is in equilibrium with the solid phase. The lower the temperatures, the thinner the layer of the liquid phase on the surface.

3. The dependence of melting temperature of nano-scale systems on size

The appearance of a liquid layer on the surface of crystalline semi-infinite objects or macro-objects at temperatures substantially lower than the reference temperature of melting has virtually no effect on the behavior of these systems. But considerable temperature range of the heterogeneous melting process leads to the fact that equilibrium temperature of low-scale systems can alter substantially as the size decreases.

For systems having the size (diameter of nano-crystal, thickness of thin film) of several dozens nanometers the equilibrium temperature of melting in accordance with (7) and (10) can fall by hundreds of degrees lower than the equilibrium melting temperature of volumetric matter T_{∞} .

Analyzing expression (7) one can come to conclusion that the value of melting temperature decline is defined by three causes. First and foremost of these causes is reduction of specific surface energy σ as a result of phase transition from solid to liquid state. The second cause is the possibility of the nano-object A surface area contraction as a result of phase transition from solid to liquid state. This cause is dependent on the first one, since the alteration of form in crystalline state is virtually impossible. But this possibility appears in liquid state, when such property as fluidity emerges. As a result, the main mechanism of mass transfer is no longer the diffusion resulting from heat-driven movement of atoms, but the movement of atoms by means of the force of surface-tension. The third cause that becomes noticeable if the first two causes are present is the reduction of the quantity of heat required for melting relating to the phase transition $\Delta H(T)$, if the melting process begins at a lower temperature due to the first two causes. In other words, at temperatures lower than T_{∞} , the system requires a lesser quantity of heat to change from solid state to liquid one.

Taking into account the aforesaid, all nano-scaled systems can be conventionally divided into two groups. To the first group belong systems that do not possess the possibility of changing their form. Consequently, the reduction of the temperature of melting for these systems is due to the first cause alone. To the second group belong systems that can change their forms. As a result, for these systems temperature falls due to the combined effect of all three causes.

To the first group belong systems in which the reduction of surface energy is possible only due to the transition from solid state to liquid state. This group includes nano-clusters and nano-crystals in free state that have the optimal form considering the ratio of surface area to volume. Furthermore, to this group also belong threadlike nano-crystals (nanowires) inside another solid phase and thin films, confined from above and below by thick layers of other solid materials. These systems do not have optimal forms and are not in free state, thereby they cannot change their form during melting.

To the second group belong systems that can change their form in the process of melting. An example of such process is the process of melting-dispersion of a film into drops. The energy expediency of this process is shown in Fig. 3, which illustrates the result of the calculations regarding the change of the surface area of a system consisting of a set of spherical objects depending on their radius. It is assumed that the volume of the system is constant, so if the radius of the spherical objects are changed, that leads to a corresponding change in their number. The character of dependence points to the fact that the increase of the size of the spherules leads to significant decrease of the surface area of the system. That way, if a system which contains $1,9 \times 10^9$ spherical objects with 10 nm radius each changes to the state of $1,5 \times 10^4$ objects with 500 nm radius each (given that $V = \text{const}$), the surface area, and, consequently, the absolute surface energy change 50-fold. For comparison, in the first group of systems the characteristic values of alteration of surface energy during the transition from solid to liquid state can amount to from 1.3 to 2-fold.

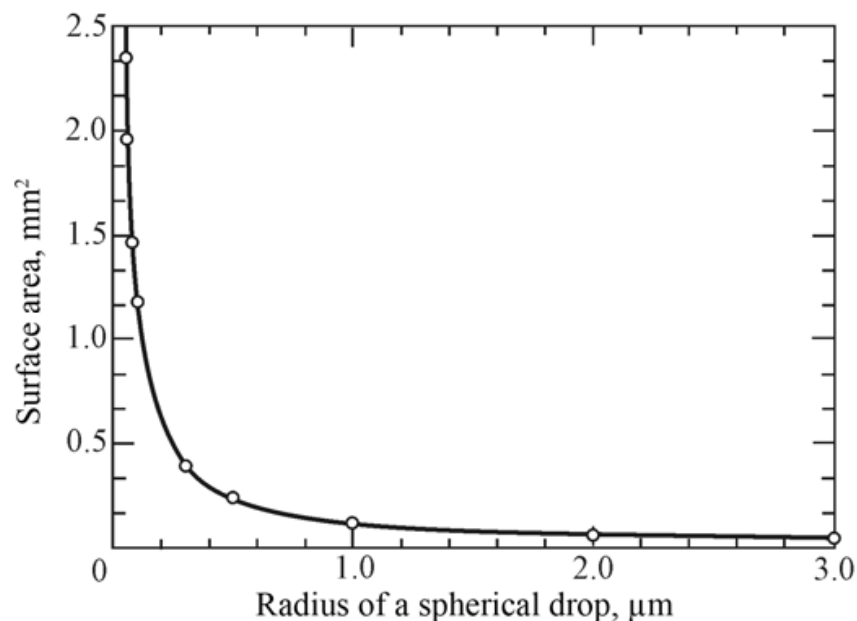


Fig. 3. Calculations regarding the change of the surface area of an array of spherical drops depending on their radius.

Along with the surface area alteration possibility, a significant effect can also be brought by noticeable differences in temperature dependencies of thermal capacities of solid and liquid phases. As it is illustrated in Fig. 4, where nickel is used as an example, ΔC_p of phase transition is less if it occurs at some temperature T_i lower than T_∞ . The consequence is temperature dependence ΔC_p and $\Delta H(T)$ of phase transition.

Consequently, for systems belonging to the second group an additional noticeable reduction of melting temperature can be expected as compared to the systems of the first group.

3.1 The dependence of melting temperature of nano-scale systems on their size without the change of form (nano-crystals, nano-clusters in free state)

If nano-clusters and nano-crystals are in free state and have an optimal form considering the ratio between surface area and volume, then they virtually don't change their form during melting. If we assume that the form of nano-crystals is close to being spherical, it is easy to see that for this kind of systems the expression (7) is transformed into

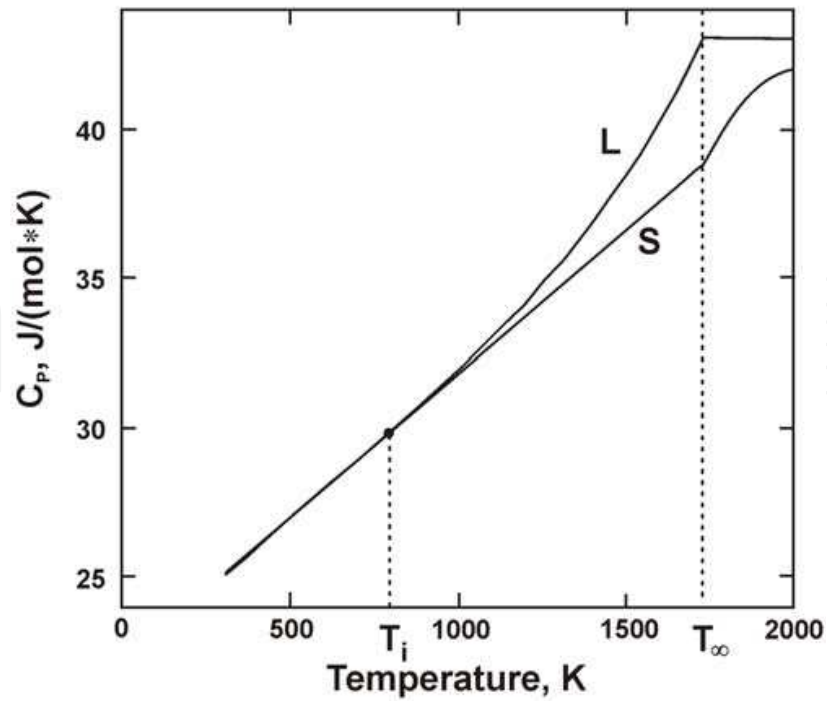


Fig. 4. Temperature dependence of specific thermal capacity of nickel in solid and liquid state.

$$T = T_{\infty} \left(1 + \frac{3\Delta\sigma}{r\Delta H(T_{\infty})} \right) \quad (11)$$

where r is the radius of the nano-crystal.

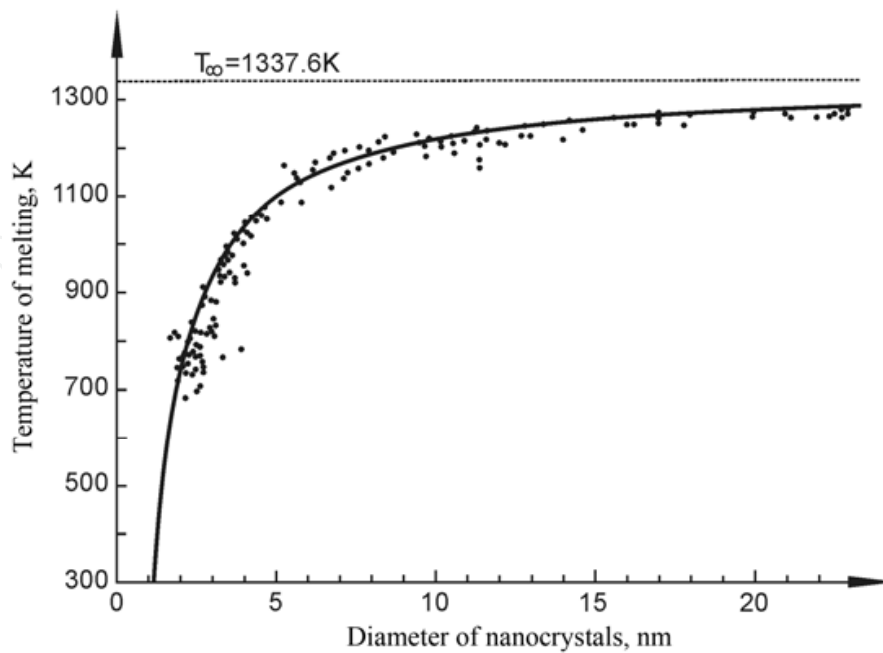


Fig. 5. Experimental values and calculated curve of dependence of gold nano-crystals melting temperature on their size according to (11).

As an example we shall calculate, using (11), the dependence of equilibrium melting temperature of gold nano-crystals on their size and compare the results of the calculations with available experimental data. The following surface energy values of gold bordering on a vacuum were taken: $\sigma_s=1.325 \text{ J/m}^2$ and $\sigma_L=1.125 \text{ J/m}^2$. The molar melting heat of gold is $\Delta H(T_\infty)=12.68 \text{ kJ/mol}$, consequently the melting heat of a unit of volume of gold which is required for substitution into expression (11) amounts to $1.243 \times 10^9 \text{ J/m}^3$. Fig.5 illustrates the array of experimental values of melting temperature of gold nano-crystals depending on their size obtained by Ph.Buffat and J.-P.Borel, as well as the calculated dependence of melting temperature according to expression (11). As can be seen, the calculated curve coincides well with the experimental data. Therefore, expression (11) reflects the experimental observations quite well.

3.2 Dependence of nano-scale system melting temperature in free state on their dimensions with changes of their state (thin films)

The peculiarity of the second group, which is represented by thin films in free state is that due to large surface area they are not optimized as far as minimum energy is concerned. From the analysis given in the Section 2 follows that the equilibrium temperature of thin films melting on inert surface is the temperature, at which thickness of the molten layer is equal to that of the thin film, and according to observations, in reality, it instantly disperses into drops. Due to this process surface energy sharply declines because of shrinking surface area – this implies optimization of shape. Experimental investigation implies that due to this factor temperature of thin films melting considerably differs from that of extensional objects, if compared to nano-crystals in free state. Temperature of Cu film melting (thickness-100 nm) on SiO_2 is below the reference temperature of melting of extensional Cu for 340 K, and the temperature of Ni film melting (thickness-100nm) on SiO_2 differs from the reference temperature of extensional Ni melting for 625 K.

The difficulty of melting temperature calculation for the second group according to formula (7) is that it includes the heat of melting $\Delta H(T)$ which itself depends on the melting temperature.

Excess absolute surface energy of a nano-scale object and possibility to lower it as a result of transition from solid to liquid state and decrease in the surface area is a kind of “trigger” for the process of melting at lower temperature. Due to this it is possible to find the temperature of a certain nano-object melting by means of iterations – in successive and multiply repeated calculations of melting temperature value T and corresponding heat of melting $\Delta H(T)$.

The first step is calculations of T according to (7). Next $\Delta H(T)$ is calculated at temperature T obtained at the first step according to the Kirchhoff equation

$$\Delta H(T) = \Delta H(T_\infty) + \int_{T_0}^T \Delta C_p dT, \quad (12)$$

where ΔC_p is the change in the heat capacity caused by the transition from solid to liquid state. The $\Delta H(T)$ value obtained is substituted into (7), and the melting temperature T is again calculated. Calculations are repeated until the melting temperature T ceases to change. This value is taken to be the melting temperature of the thin film of the selected thickness. In order to obtain the melting temperature of a thin film of another thickness, volume V substituted into (7) is corrected according to thickness changes and the calculations are repeated.

Theoretical curves of Cu thin films melting temperature are calculated according to their thickness by means formula (9) and by means of described iteration method using formulae

(7) and (12) as well. The object of modeling is a copper film area with surface $1000 \mu\text{m}$ in diameter deposited on the surface of tungsten. The following initial data are used. For the free upper copper film surface, we use $\sigma_S = 1.72 \text{ J/m}^2$, and for the lower film surface bordering on tungsten, $\sigma_S = 2.83 \text{ J/m}^2$. This value occurs theoretically only, when σ_S equals the surface energy of tungsten. It is assumed that in calculations according to (7) and (12) the film disperses into spherical drops $3 \mu\text{m}$ in diameter as a result of melting; each drop touches the surface of tungsten at a single point, and $\sigma_L = 1.265 \text{ J/m}^2$ therefore corresponds to the surface energy of liquid copper. We assume that the volume of copper does not change as a result of melting and dispersion. The molar heat of copper melting is $\Delta H(T) = 13 \text{ kJ/mol}$, hence heat of melting per volume unit necessary for (7) or (12) is $1.826 \times 10^9 \text{ J/m}^3$. The calculated curves are compared with the experimental melting temperatures of different thin copper films shown in Fig. 6.

It is noteworthy that experimental melting temperature of a rather thick film of 100 nm is considerably lower than that of bulk Cu ($\sim 160^\circ\text{C}$). If we go back to Fig.5, we notice that the melting temperature of gold nano-crystals (the diameter of gold nano-crystals is significantly smaller – 20 nm) differs from bulk gold melting temperature by 80°C .

Curve 1 demonstrates calculations according to (9) which does not take into consideration possibility of form alteration and heat of melting. We can see that this curve lies well above the experimental values – i.e. in case the surface area remains unchanged during the process of melting, the dependence of the thin film melting temperature will be closer to that of bulk melting temperature. Thus, formula (9) cannot describe temperature changes of melting accompanied by the dispersion of a film into drops.

Curve 2 obtained iteratively with the use of (7) and (12) shows the inclusion of the temperature dependence of the heat of melting and a change in the surface area of the system caused by its dispersion into drops decreases the melting temperature. Curve 2 is much closer to the experimental values.

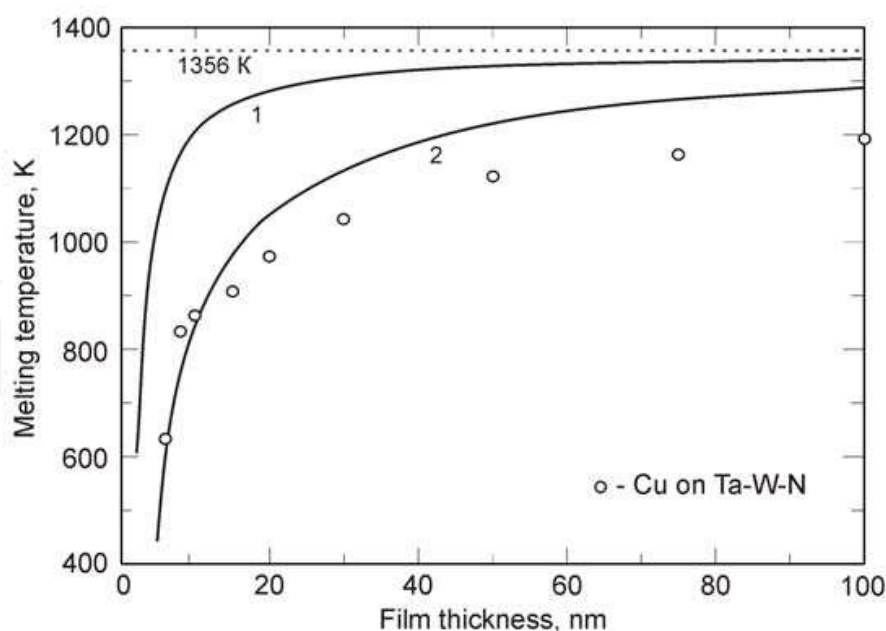


Fig. 6. Experimental Cu thin film melting temperatures on the surface of amorphous alloy Ta-W-N and calculated Cu thin film melting temperature dependencies on their thickness on the surface of tungsten. Curve 1- calculation according to (9), curve 2 – calculations by the iteration method according to (7) and (12).

As with copper, we calculate the film thickness dependence of theoretical melting temperatures of nickel thin films by the same iterative procedure with the use of (7) and (12). The calculations are made for nickel films on Al_2O_3 surface. We take $\sigma_s = 1.86 \text{ J/m}^2$ for the free upper surface of nickel films and $\sigma_s = 2.6 \text{ J/m}^2$ for the lower surface bordering on Al_2O_3 . As with copper, it is assumed that melting causes film dispersion into spherical drops $3 \mu\text{m}$ in diameter, which touch the surface at a single point each; we therefore use $\sigma_L = 1.62 \text{ J/m}^2$, is liquid nickel surface energy. The molar melting heat of nickel is $\Delta H(T) = 17.6 \text{ kJ/mol}$, its molar volume is 6.6 cm^3 , and the heat of nickel melting is therefore $\Delta H(T) = 2.67 \times 10^9 \text{ J/m}^3$. We use the temperature dependence of the heat capacity of solid to liquid transition for bulk nickel

$$\Delta C_p = 4 - 0,003T + 5,1 \times 10^{-6}T^2 - 1,5 \times 10^5 T^{-2} \quad (13)$$

obtained from the data represented in fig.4.

Fig. 7 shows that the dependence calculated for nickel films on Al_2O_3 (curve 1) lies slightly above the experimental melting temperatures, as in the case with copper.

Further we analyze possible reasons for the observed deviations of the theoretical film thickness dependences of the temperatures of fusion obtained using the procedure suggested above from the experimental dependences.

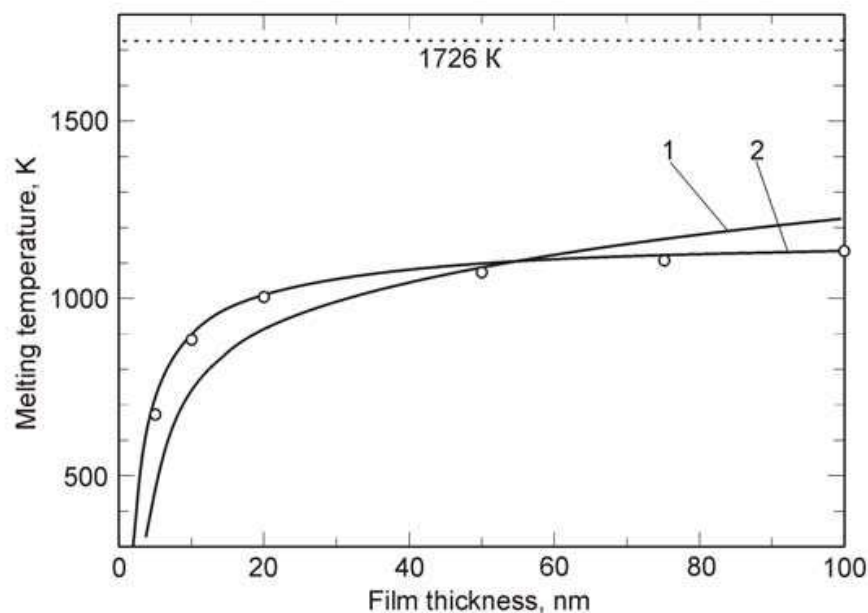


Fig. 7. Experimental and theoretical film thickness dependencies of melting temperature of thin nickel films calculated by the method of iterations according to (7) and (12). Curves (1) and (2) were calculated for Ni on Al_2O_3 from the data using the $\Delta C_p(T)$ dependence for volume nickel (Eq. (13)) and dependence (14), respectively.

The conclusions that can be drawn from our study of the contributions of the terms present in (7) to changes in the temperature of fusion of a system whose absolute surface energy can change as a result of shape changes are the following:

- contribution of changes in the surface energy to a decrease in the temperature of fusion is determined in (7) by the difference $T_\infty(\sigma_L A_L - \sigma_s A_s) / (\Delta H(T_\infty) V)$. Since $\sigma_s A_s T_\infty / (\Delta H(T_\infty) V) \gg \sigma_L A_L T_\infty / (\Delta H(T_\infty) V)$, $\sigma_L A_L T_\infty / (\Delta H(T_\infty) V)$ does not make a significant

contribution. It follows that the size of drops and their shape influence changes in melting temperature insignificantly; i.e. the dispersion of a thin film into drops itself is of importance, but it does not matter whether these drops are ideally or non-ideally spherical and 1 or 5 μm in diameter.

- At the same time, $\sigma_s A_s T_\infty / (\Delta H(T_\infty) V)$ makes a substantial contribution. It follows that the initial energies $\sigma_s A_s$ of the upper and lower (at the boundary with a different material) thin film surfaces make a substantial contribution to melting temperature decrease.
- term $\sigma_s A_s T_\infty / (\Delta H(T_\infty) V)$ makes the most significant contribution because of different temperature dependences of the heat capacities C_p of the liquid and solid phases. The temperature dependences of the heat capacities of the liquid and solid nickel phases are shown in Fig. 4. The larger this difference, the larger the contribution of this term to a decrease in the temperature of fusion.

It follows from these conclusions that there can be several reasons for deviations of the theoretical curves calculated in this work from the experimental data.

The first reason for these deviations is the use of the temperature dependences of the heat capacities of volume liquid and solid phases in integration according to (12).

It follows from the introduction that the amplitude of oscillations of crystal atoms situated close to the surface is larger by than in the bulk. As a consequence, the Debye temperature of surface layers is lower by than that of the bulk material. Since the heat capacity is related to the values specified in accordance with the Debye quantum theory of heat capacity, the heat capacity of surface layers should be higher than the heat capacity of bulk materials. The amplitudes of atomic oscillations are higher in the liquid than in the solid phase, and the temperature dependence of the heat capacity of the liquid phase is in the majority of cases steeper compared with the solid phase. Extending this conclusion to the surface layer, we are led to suggest that the difference between the temperature dependences of the heat capacities of the surface layer in the liquid and solid state (that is, $\Delta C_p(T)$) increases compared with the bulk material.

It should in addition be noted that it follows from the same reasoning concerning the difference in the phonon spectra between the surface layer and volume phase that the heat capacity of the surface layer depends on film thickness as long as the film thickness is comparable with the surface layer thicknesses at which the amplitudes of atomic oscillations differ from those in the bulk.

Based on these considerations, we corrected the coefficients of the temperature dependence $C_p(T)$ to fit the calculated dependence of melting temperature to the dependence observed experimentally for the thin nickel film on Al_2O_3 . The results are shown in Fig. 7 (curve 2). The corrected dependence has the form

$$\Delta C_p = 4 - 0,0128T + 13,7 \times 10^{-6} T^2 - 1,5 \times 10^5 T^{-2} \quad (14)$$

The second reason for the deviations can be the accuracy of the surface energy σ_s values that we use. The reliability of surface energy values leaves much to be desired because of the problems related to their measurement. The question of what energy value should be used for the interphase boundary between two materials remains open. What is more, we use a constant surface energy value, whereas, like ΔH , it depends on temperature. The discrepancies between the calculated curve (Fig. 6, curve 2) and experimental data on copper can therefore be caused by the use of the σ_s value for tungsten in our calculations, whereas the experimental data on the copper film were obtained on a Ta-W-N amorphous alloy whose surface energy is unknown but is likely higher than that of tungsten.

There is one more reason, if the first one is not responsible for the deviations. This is the accuracy of the temperature dependences of the heat capacity C_p of the solid and liquid phases. Calculations show that, for instance, a 10% error in the temperature dependence for liquid copper toward an increase in its heat capacity results in a noticeable (by about 50 K) shift of the calculated film thickness dependence of melting temperature toward lower temperatures.

3.3 The dependence of melting temperature of nano-scale systems on their size without form alteration (nanowires within other solid material)

As one more example of systems, relating to the first group, one can exemplify the melting of In, Cd and Zn nanowires within porous Al_2O_3 .

Porous anodic alumina (PAA) is a closely packed structure, consisting of many hexagonal cells, in the center of which is a vertical pore. PAA attractiveness is in its low range of pore sizes in diameter and this size is well controlled in the course of its formation. Deposition of In, Cd and Zn in these pores is implemented by electrochemical method using pulsed deposition, which ensures a void-free PAA pore filling by metal.

Fig. 8 illustrates scanning electronic microscopy (REM) photography of some porous element, where nanowires of In are deposited in its pores. As it follows from the results of microscopy, metal homogeneously fills these pores and metallic wires have no voids. That is why the diameter of nanowires can be considered equal to that of pores in anodic oxide.

Melting temperature of In, Cd and Zn metallic nanowires is defined by means of differential scanning calorimetry (DSC) and with the help of incipient thermal absorption, which is expressed in DSC graphics as deviation from the linear law. Phase transitions aren't discovered in initial structures of PAA without a deposited metal at temperatures from 323K to 773K, therefore observed thermal absorption in objects with a metal deposition may have been caused only by the process of melting.

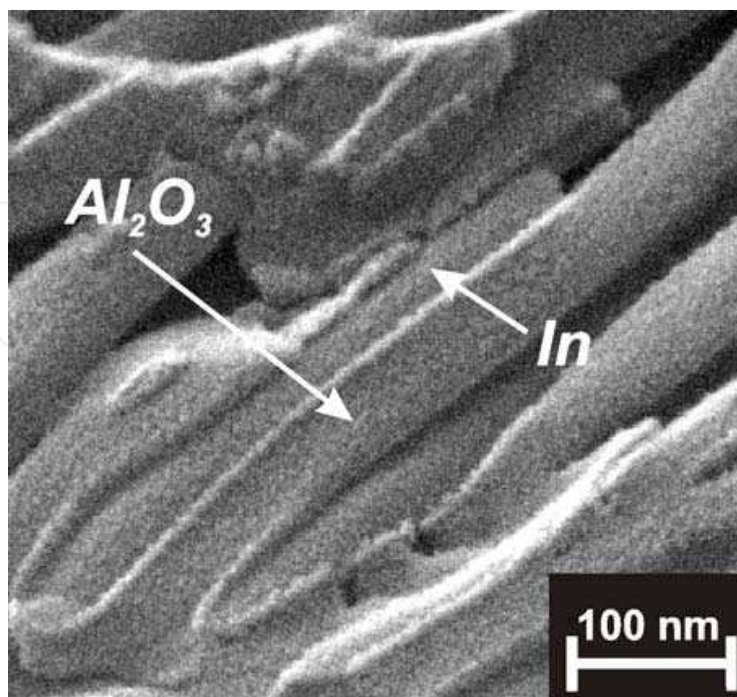


Fig. 8. SEM photographs of In nanowires in porous alumina host.

Fig. 9 illustrates an observed dependence of melting temperature of In nanowires in pores of different diameter. As we can see, along with a downscale of nanocrystals to 30 nm melting temperature reduces. Nevertheless, with the reduction of size to 20 nm, the increase of melting temperature takes place. Fig.9 draws attention to the fact that the reduction of melting temperature of nanowires, enclosed in PAA host, is inconsiderable (3K), unlike in the previous cases. This dependence is not only the feature of In nanowires. This type of so-called non-monotonous dependence is also observed for Cd and Zn nanowires.

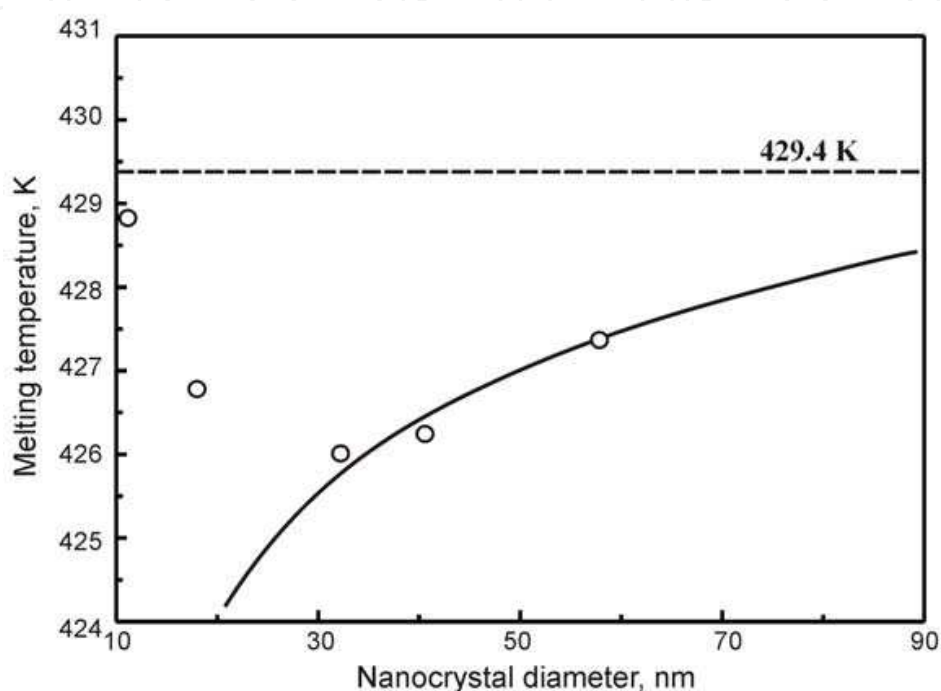


Fig. 9. Experimental melting points of In nanowires in PAA and estimated dependence of melting temperature using the equation (15).

Formula (7) enables us to calculate temperature dependences of melting for In, Cd, Zn nanowires. The length of cylinder is expected to remain unchangeable, and its diameter ranges from 8 to 20 nm. As the diameter of nanowires is much less than its height, it means that the calculation of surface area is added up to determining of the cylindrical surface. Taking into account the impossibility of nanowire shape alteration in PAA, (7) transforms into

$$T = T_{\infty} \left(1 + \frac{2\Delta\sigma}{r\Delta H(T_{\infty})} \right) \quad (15)$$

Initial data required for calculations are represented in Table 1. Since temperature dependences C_{pL} and C_{pS} of In coincide, ΔC_p equals zero in this case.

As it is shown in Fig.9, the calculated curve coincides with experimental values at reducing In nanowire diameter to 30nm. The same coincidence of calculated and experimental data in the same range are obtained for Cd and Zn.

These derived temperature dependences prove that when there is no possibility to alter surface area, the reduction of melting temperature (systems of the first group) with a size changing is very little. The crucial moment is this: temperature dependence $\Delta H(T)$ of systems relating to the first group doesn't make any impact on the reduction of melting temperature.

Material	σ_s , mN/m	σ_L , mN/m	T_{∞} , K	$\Delta H(T_{\infty})$, J/m ³ × 10 ⁹	ΔC_p
In	633	556	429,4	0,42	0
Cd	606	560	593,9	0,47	-8,99-0,0258T-1,79 ⁻⁵ T ² +2,63 ⁵ T ⁻²
Zn	830	767	692	0,78	21,2-0,13T+4,9 ⁻⁵ T ² -8,55 ⁵ T ⁻²
Al ₂ O ₃	2600				

Table 1. Initial data for the calculation of melting temperature of In, Cd and Zn nanowires.

From our point of view, the reason for the increase of melting temperature in nanowires with diameter < 30 nm is not grounded in an amount of substance, that in this case doesn't correspond a physicochemical notion "phase", as it was remarked in Section 2. This range of sizes is influenced by the neighboring material. The analysis of causes of melting temperature increase with size reduction of 20 nm is examined below.

4. The role of heterogeneous melting in various physical and chemical processes

The analysis, presented in the previous sections, shows that if there is a surface, there are reasons of thermodynamic and energy character, which determine the reduction of melting temperature in low-sized objects along with the decrease of their dimensions. However, a considerable temperature of heterogeneous melting results in becoming of this kind of melting as an initiator or participant of other processes in low-scale systems and thus it makes a significant influence on their behavior.

4.1 The behavior of thin films on inert substrates

As it is stated above, thermal treatment of thin films from a few to hundreds of nanometers in thickness, deposited on an inert substrate (i.e. having no chemical reaction with it) leads to its micron-sized droplets decay.

The study of various material thin films (in particular Cu, Au, Ag, Ni, Fe) of different thickness has demonstrated that this process has no strictly determined temperature. It can occur in some temperature range, but its temperature is substantially lower than that specified in a reference book of a three-dimensional material.

For instance, copper film 20 nm in thickness starts to disintegrate into drops at 883 K after 300 s, while at 743 K this process appears after ~13000 s. The film 100 nm in thickness begins to dissociate at 1013 K after 420 s, while it also dissociates at 913 K, but after ~9000 s. The disintegration of copper thin film occurs locally at any place of the sample and then spreads further frontally (Fig.10). As a result, it is possible to distinguish three sample areas: the area where the film remains continuous (Fig.10 (a)); the area where the film is totally dissociated into droplets (Fig.10 (e)), and the third one - narrow area or a front, where dispersion takes place (Fig.10 (b-d)).

Fig.11 represents dependences of time to melting on annealing temperature for copper films of different thickness. These experimental points are perfectly approximated (with correlation ratio 0,98-0,99) to the following equation

$$t = \frac{A}{\exp\left(\frac{E_{act}}{RT}\right)} \quad (16)$$

which follows the Arrhenius equation.

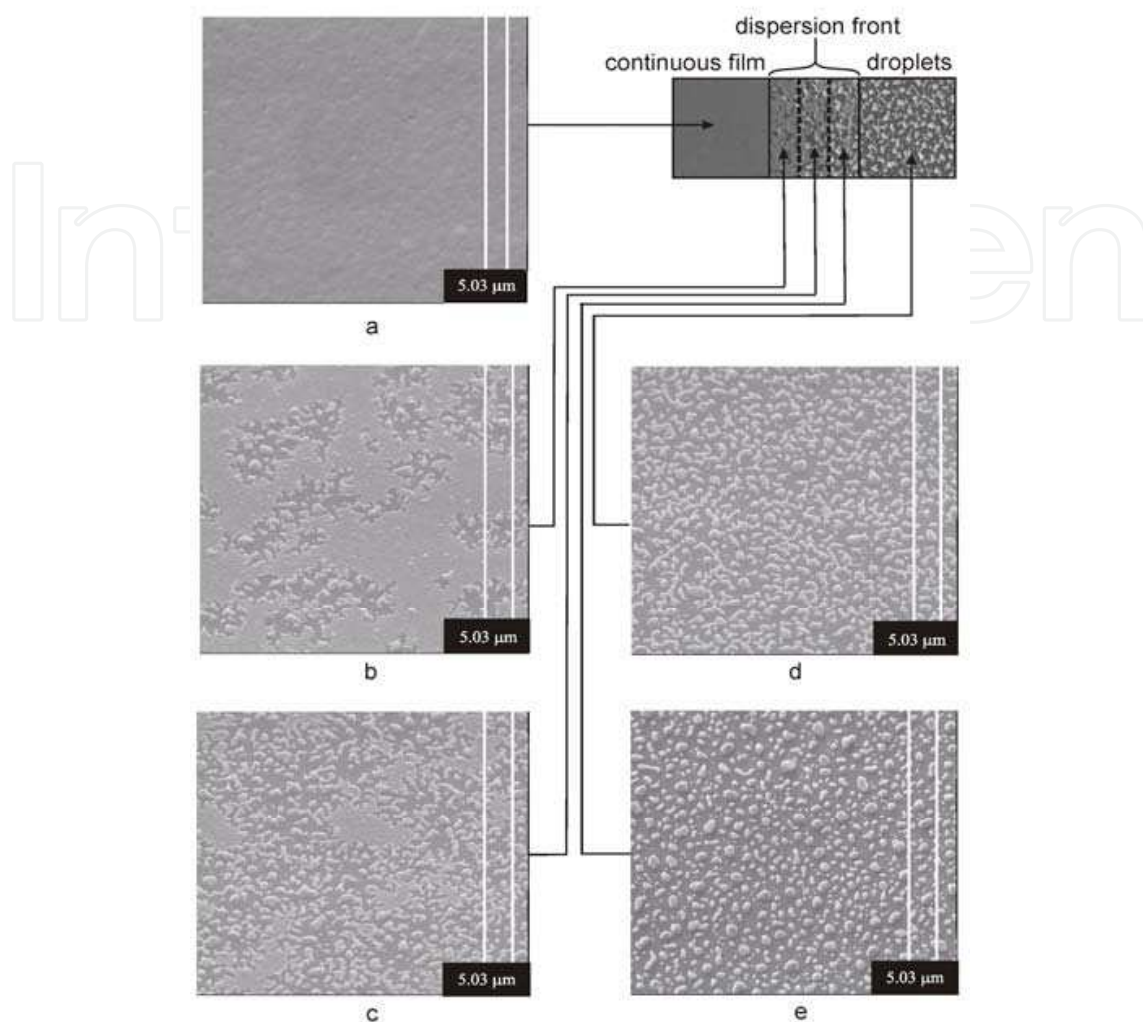


Fig. 10. SEM photographs of the copper thin film at different stages of melting: a) region of continuous film; b) - d) region, where melting of film occurs; e) region, where this film dissociated into droplets.

This approximation of experimental data enables to calculate activation energy of melting-dispersion for films of different thickness. In accordance with these calculations, E_{act} varies from 120 to 260 kJ/mole depending upon copper film thickness. For example, dependence $t=f(T)$ for copper film 100 nm in thickness is approximated by means of this equation:

$$t = 1 \cdot 10^{-11} \cdot \exp\left(-\frac{260 \cdot 10^3}{8,31 \cdot T}\right) \quad (17)$$

Since this type of dependence is also common for diffusion, one can presume that the observed phenomenon is of diffusion nature. In this case diffusion coefficient D_0 , calculated from (17), is equal to $\sim 10000 \text{ cm}^2/\text{s}$, that is two orders of magnitude more than specified in reference books copper self-diffusion coefficient, which is $70 \text{ cm}^2/\text{s}$.

Values E_{act} and D_0 obtained are similar to the ones experimentally defined by A.E. Dolbak and his colleagues, who studied copper diffusion from its thin strips $\sim 12 \text{ nm}$ in thickness

along pure silicon surface. This high diffusion coefficient D_0 is explained in terms of surface diffusion that occurs via the solid - state spreading or “unrolling carpet” mechanism.

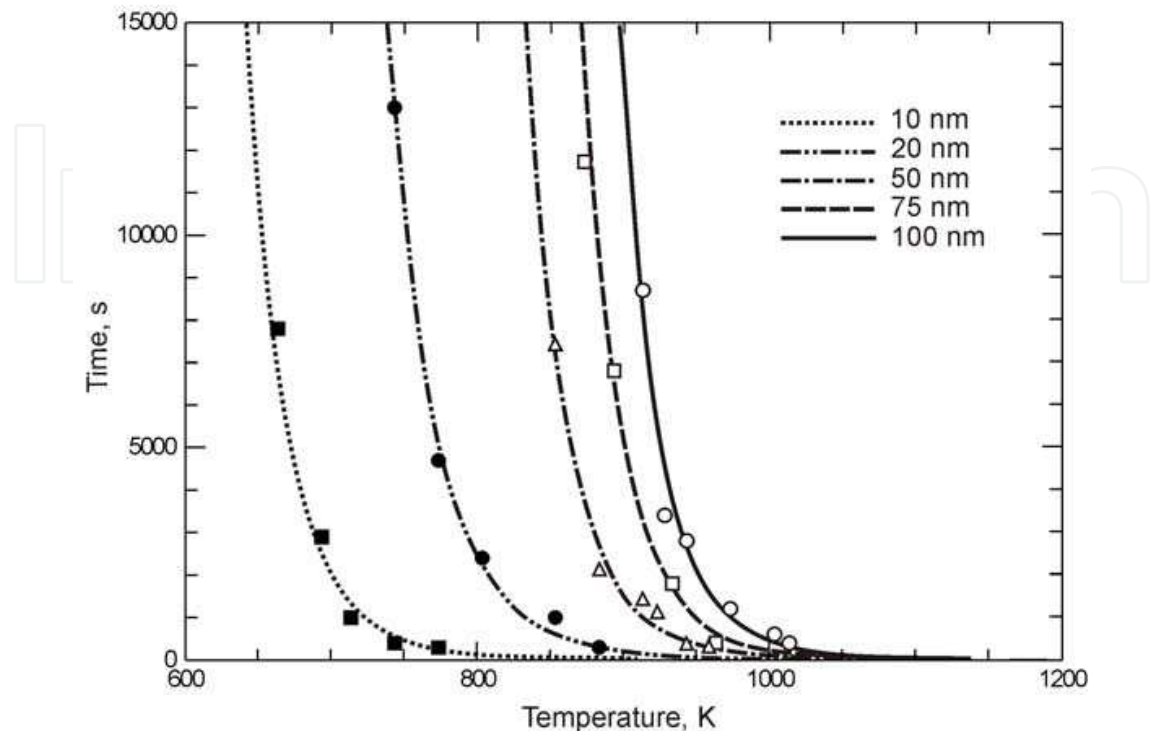


Fig. 11. Dependences of melting time in copper thin films of various thickness on heating temperature in a vacuum.

That's why it seems quite sensible to explain the dissociation of thin film into droplets by surface diffusion. But it does not seem to be correct. Diffusion is defined to be a mass transfer as the result of thermal movement of substance particles in the direction of their concentration decrease. Volume diffusion results in their uniform and even distribution of particles throughout the volume and surface diffusion - over the surface. In this case we deal with quite an opposite effect: the process goes from the uniform surface distribution of particles to their collecting into droplets, i.e. in the direction of concentration increase.

At the same time, we should draw attention to the following issue. Fig.12 demonstrates the area, defined experimentally depending upon the thickness where dispersion of nickel thin film can be observed. The upper bound of shaded area is the dependence of dispersion temperature, where it begins after 5s. The lower one shows when the same process begins after 5 h. Curve 1 illustrated on Fig.12, is an estimated dependence, attained by iteration method, using equations (7) and (12), which is shown on Fig.7 (Section 3.2). As we can see, the estimated dependence is almost wholly situated in the shaded area of experimental observations.

Furthermore, if we try to employ a theoretical dependence in the area of film heavy gages, it seems rather unusual. In compliance with this dependence, a rather thick film 0,5 - 1,0 μm in thickness is to melt at 300 - 400 K below than that specified in a reference book. Fig.13 represents photomicrographies of iron film surface at 1323 and 1273 K, which are similar to nickel regarding its behavior. Comparison of Fig.13 (a) and (b) enables us to assume that film 0, 5 μm in thickness after its annealing at 1323 K had such a morphology that could be formed only with a liquid phase, thus it confirms calculations result.

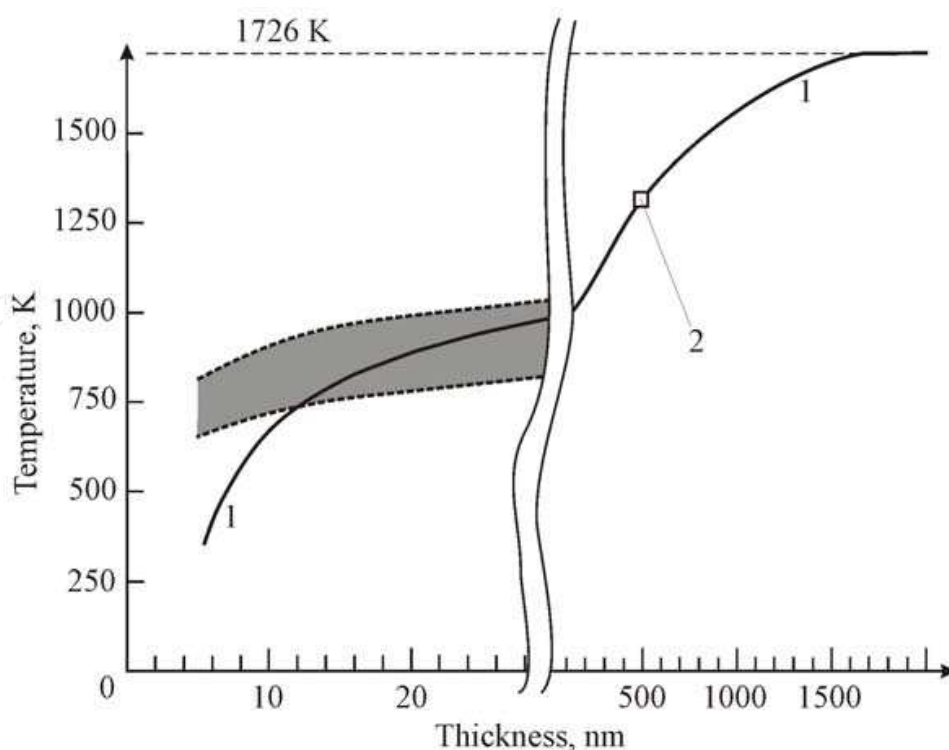


Fig. 12. Temperature range, where dispersion of nickel thin film in droplets is observed, and calculated curve of melting temperature dependence of nickel thin films on its thickness. Curve 1 - calculation by means of iteration method using formulas (7) and (12); 2 - control data point.

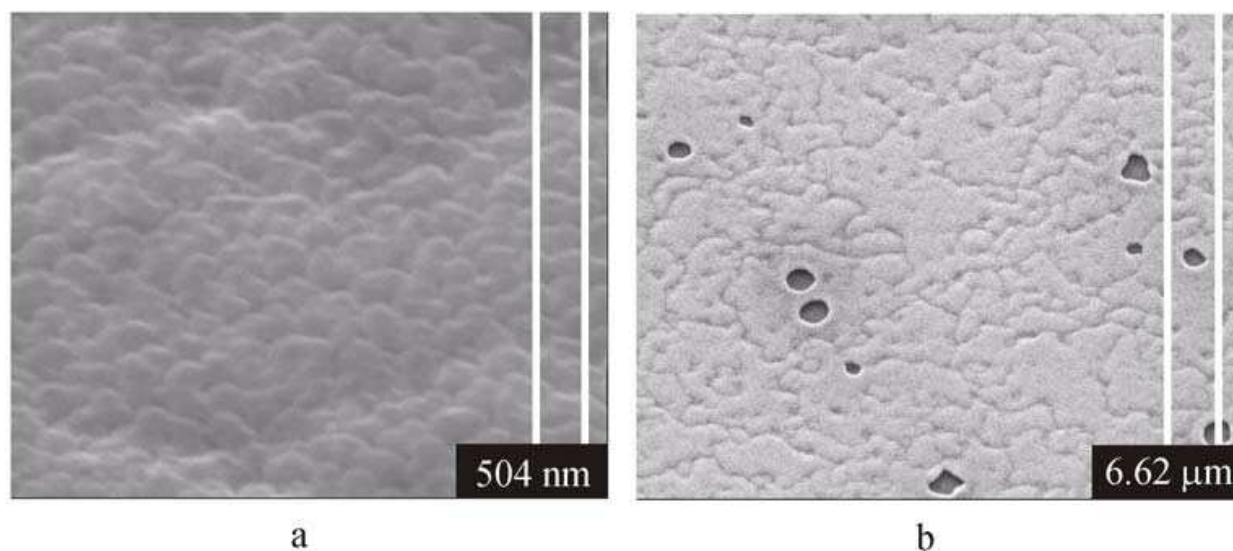


Fig. 13. SEM photographs of the iron film 0,5 μm in thickness: a) - after annealing at 1273 K; b) - after annealing at 1323 K

There is an opinion that these facts are just coincidence, as the process of dispersion is a purely kinetic one and its usage for description of equilibrium thermodynamics relationships is not quite justifiable. Moreover, this process is an irreversible that gives evidence of its non-equilibrium state.

However, it is necessary to remember (Fig. 2) that in a semi-infinite system, where the heterogeneous melting occurs, the equilibrium melting temperature is a temperature at which the crystalline phase disappears completely. But the surface causes the emergence of the liquid phase long before this temperature is achieved. Similarly the equilibrium melting temperature of a thin film described by expression (7) is a temperature at which the whole film turns liquid but virtually the liquid phase on the film surfaces arises even earlier. Thus, theoretical curve 1 in Fig. 12, derived from expression 7, indicates that there are objective energy (i.e. thermodynamic) reasons producing a considerable displacement of equilibrium between liquid and solid phases towards a lower temperature as a thin film thickness is decreasing. In fact, owing to the heterogeneous melting the liquid phase and the thin film dispersion into droplets, caused by this phase emergence, arise even earlier at lower temperatures. Curve 1 in Fig. 12 should have coincided with the upper boundary of the shaded area.

If this process depended on kinetic laws only, we should have expected the film structure to affect the temperature and dynamics of this process significantly. However, the study of the thin copper films 50 nm thick on the Al_2O_3 surface showed the following: the temperature range, within which films with an average grain size of 90 nm disperse, is 10-20 K higher than that for the films with a grain 25 nm thick. Such an insignificant difference also shows that despite the evident importance of kinetics (exponential dependence of process rate), the dispersion process results from thermodynamics to a greater extent.

Kinetic peculiarities of the thin film dispersion into droplets may be conditioned by such liquid properties as viscosity or fluidity and by evaporation, all of them highly dependent on temperature.

Thin silver film behaviour during the annealing was studied. It was found (Fig. 14) that the material mass decreases with time, diminishing most intensively during the first 15-20 minutes of high-temperature exposure.

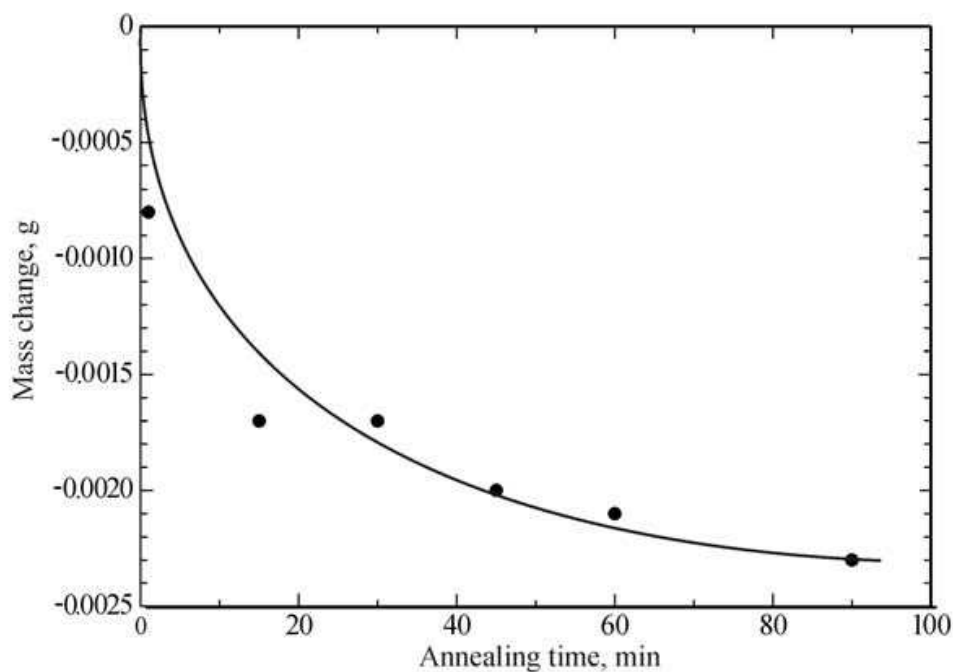


Fig. 14. The dependence of thin silver film mass variation (630 nm thick) versus the annealing time at temperature 820 °C.

The results of this experiment indicate that during the melting-dispersion process of a thin film into droplets a part of a substance evaporates. Moreover, we were able to observe a mass loss even at the temperature lower than the equilibrium melting temperature but at which the process of dispersion into droplets occurs.

The information described allows us to assume the following mechanism of the thin film dispersion into droplets. This mechanism accounts for the absence of a particular temperature of this process. Thin film excess surface energy causes this process. To reduce surface energy, we can decrease specific surface energy σ and thin film surface area A . But surface area shrinkage in a crystalline state is extremely complicated. Because of this, during heating the heterogeneous melting occurs faster.

On the upper and lower thin film surfaces there arises an inherent liquid phase that wets well and partially (not always completely) dissolves crystal grains of the thin film on the boundaries (Fig. 15 (a)). According to the experimental results obtained by AFM a thin film, e.g. 50 nm thick, consists of no more than two layers of crystalline grains. Liquid layer thickness depends on temperature. For example, dispersion of a gold film 50 nm thick was observed within the temperature range 903-1003 K. Formula (10) indicates that both at 903 K and at 1003 K on the upper and lower surfaces of a thin gold film there has to exist a liquid layer of more or less uniform thickness: approximately 12 and 16 nm, respectively.

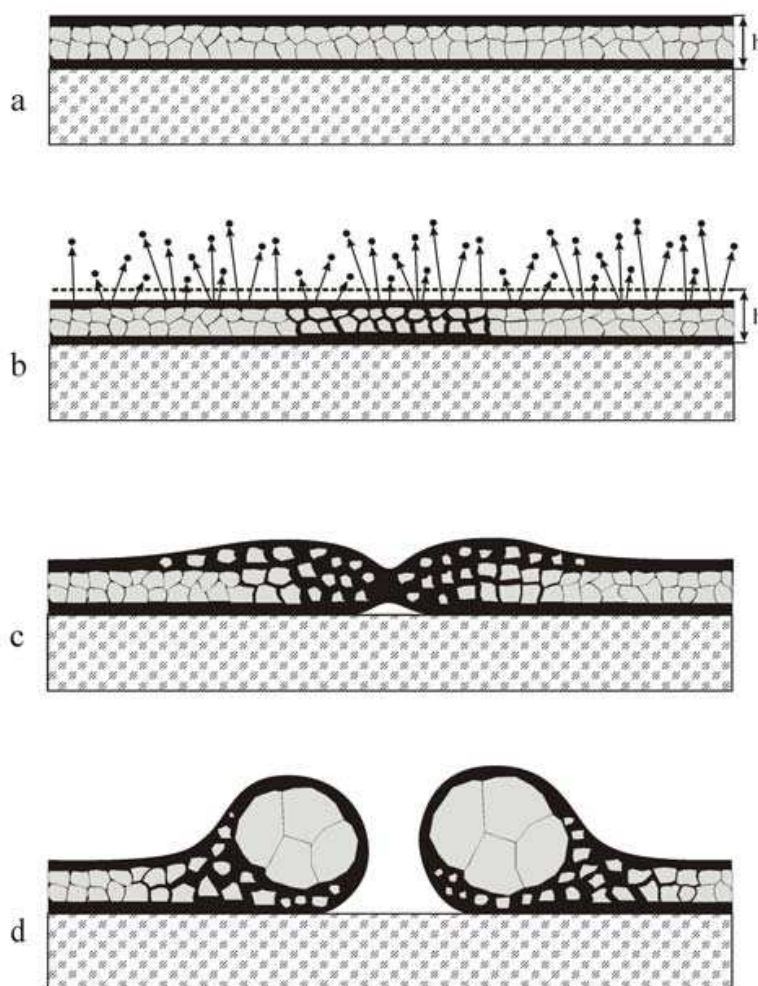


Fig. 15. Schematic diagram illustrating the melting-dispersion of a thin film on the inert surface.

As a liquid layer appears, there starts a sufficiently intensive process of evaporation. This reduces a film thickness, decreases its equilibrium melting temperature and diminishes the quantity of a solid crystalline phase (Fig. 15 (b)).

During the heating time grains with boundaries are sufficiently wetted, and in a local region the liquid phase penetrates into the entire film thickness (Fig. 15 (b)). Liquid evaporation and propagation resulting from the wetting determines the kinetic component of thin film dispersion into droplets: at higher temperatures fluid viscosity is lower and dispersion starts quickly; at lower temperatures viscosity is higher, wetting occurs more slowly, and dispersion process starting only in a while is slower.

Owing to the fact that the liquid phase is fluid, sufficiently wets its inherent crystalline solid phase and poorly wets the substrate inert surface, the surface tension force reduces the thin film surface area, spending the excess surface energy of the thin film. As a result, the liquid phase leaks on its inherent solid phase entraining crystallites it contains and causing a thin film rupture (Fig. 15 (c)). Surface energy lowering shifts the equilibrium between the liquid and solid phases towards higher temperatures, which makes impossible the existence of this amount of the liquid phase at the given temperature. Because of this, the process of liquid crystallization starts easily at the same temperature (as there is no need to spend energy to form an interface). Liquid crystallization is accompanied by a local heat release, which causes the effect of "partial melting" of the polycrystalline film remained in the solid state (Fig. 15 (d)). As a result, there arises a moving front where the melting-dispersion process occurs.

Thus, it is evident that the process of thin film dispersion is not just a melting process. However, it is quite obvious that the heterogeneous melting is the main component of this process and determines its temperature.

The studies of kinetics of thin film dispersion into droplets revealed an anomaly in the behavior of thin films less than 30 nm thick - nonmonotonic melting temperature dependence. This anomaly overlaps with the results obtained for filamentary nanocrystals (see part 3.3).

Fig. 16 (a) and (b) represents dependences of the equilibrium melting temperature and activation energy of dispersion of thin Cu, Ag and Au films into droplets. These metals belong to the same group of the periodic table. These diagrams show certain regularity. According to Fig. 16 (a), melting temperature dependences of thin films on their thickness are monotonic for Cu and Ag; but the thinner thickness, the higher melting temperature thin Au films (less than 20 nm thick) have, instead of expected temperature lowering. Besides, the diagram illustrating the activation energy dependence for Au also has a minimum on the same thickness, but activation energy falls steadily with reducing thickness for copper. Ag has an intermediate position in the group between Cu and Au in the periodic table and, thus, behaves accordingly: given the stable monotonic melting temperature dependence, the activation energy dependence obtains a minimum. I.e., Ag films 10 nm thick have higher energy of dispersion into droplets than a film 40 nm thick has. Thus, there is an evident regularity: as an atomic number of an element in a group increases, thin film dispersion into droplets is more difficult.

In section 2 we have already mentioned that there exists a problem of a physicochemical concept of "phase" for a thin film with thickness less than a certain thickness. Phase is a certain amount of substance which has an interface, and at any point of which thermodynamic functions are constants. However, as the thin film thickness reduces, both of its surfaces approach each other gradually, and at the certain moment this principle is violated and a thin film no longer corresponds to the "phase" concept.

There are three evident cases here.

The first extreme case is a characteristic feature of thick films several micrometers thick. The substrate effect is unnoticeable in this case. The film has the properties of an actually solid material and behaves like a classical thermodynamic phase, which borders upon the other phase – the substrate. The surface contribution to the combined energy of such a system is hard to notice. The film and the substrate can be viewed as two independent systems.

The second extreme case is a feature of the thinnest films and corresponds to a high degree of substrate effect. The peculiar feature of this case is that the thin film is, in essence, an adsorbed layer reducing the substrate surface energy. The thin film is not a phase in a classical physicochemical understanding. The thin film and the substrate are a single system in this case. Thin film material atoms tend to spread uniformly on the substrate surface area. According to the definition, the surface diffusion phenomenon relates to this very case.

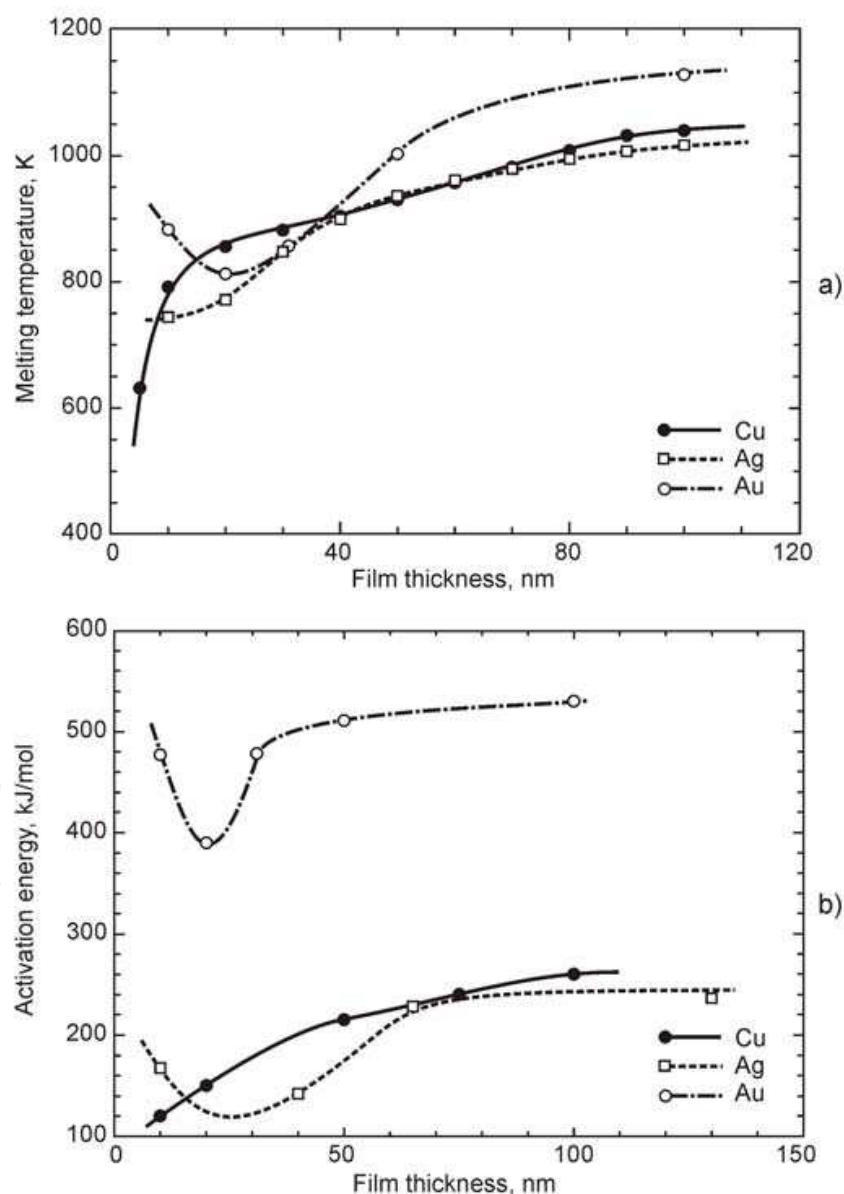


Fig. 16. The dependences of melting temperature and activation energy of thin films of Cu, Ag and Au on their thickness.

The third case is intermediate between the first one and the second one. When the film thickness exceeds the thickness of the second case, the thin film starts displaying properties of an individual independent object with its own volume and constrained by the surfaces above and below. In this case the substrate affects the film, but the film behaves like an independent thermodynamic system in non-equilibrium due to a substantial surface energy contribution. This system tends to transform into such a condition so that a volume energy distribution prevails over the surface one. As a result, the film disperses into droplets, each becoming an independent object. The fact that the thin film disperses into droplets proves it is not a phase. However, the film and the substrate can be viewed as two different systems. The transitional nature of the third case lies in the fact that the substrate effect gradually weakens and the thin film individuality increases as the thin film thickness grows. Thus, the main reason of non-monotonic dependence of melting temperature of a thin Au film and filamentary In, Cd and Zn nanocrystals on their size (thickness, diameter) is increasing effect of the material, which a low-sized system adjoins to. This is a transitional area between 2-D film shrinking into a 3-D droplet and surface diffusion and adsorption process.

4.2 Filling narrow trenches with copper

The phenomenon of heterogeneous melting of a thin film can be used for filling with copper of narrow trenches and contact windows with a high aspect ratio.

A thermal treatment at 800 °C of thin copper layer, which is conformally deposited on the structure of trenches on the surface of an amorphous Ta-W-N allow, which does not interact with it, leads to the phenomenon of dispersion of a thin film on spherical droplets accumulating mainly in the crest of the structure (Fig. 17 (a, b)). To suppress this phenomenon, the films of the Ta-W-N allow and copper are separated by a wetting layer of titanium. It is found that the titanium layer thickness up to 10 ÷ 15 nm does not change the nature of wetting and copper at the same temperatures continue to disperse into droplets, as in Fig. 17 (b). (It should be noted here that the film thickness corresponds to the thickness of the film on a flat surface. In view of the differences of deposition rate a film thickness on the sides were somewhat lower.)

However the situation changes dramatically for thicknesses of titanium layer over 15÷20 nm: wetting appears, and copper start to flow into the trenches (Fig. 17 (c)).

This result is a good indirect evidence that copper thin film at 800 °C had properties of fluid and was in liquid state: material is selected into spherical droplets, if surface wetting is absence, and fills the cavities, if there is good surface wetting.

In addition, in example of titanium layer we see again a criticality of thin film thickness up to 20 nm from point of view a physicochemical notion "phase".

4.3 Degradation of aluminum contacts to the semiconductor in silicon integrated circuits

When metallization of silicon integrated circuits was single-level and single-layer, and its material was aluminum, failures began to appear with gradual decreasing the element sizes. It was established that the reason of the appeared frequent failures of integrated circuits with the one layer aluminum metallization was the shorting of *p-n* junctions due to the heat treatment. A selective removal of the aluminum film from the substrate surface near the contact window after heat treatment at 470°C for 30 min indicates catastrophic degradation of the morphologic perfection of the contact interface in the form of deep holes in silicon, that shows SEM-micrography (Fig. 18).

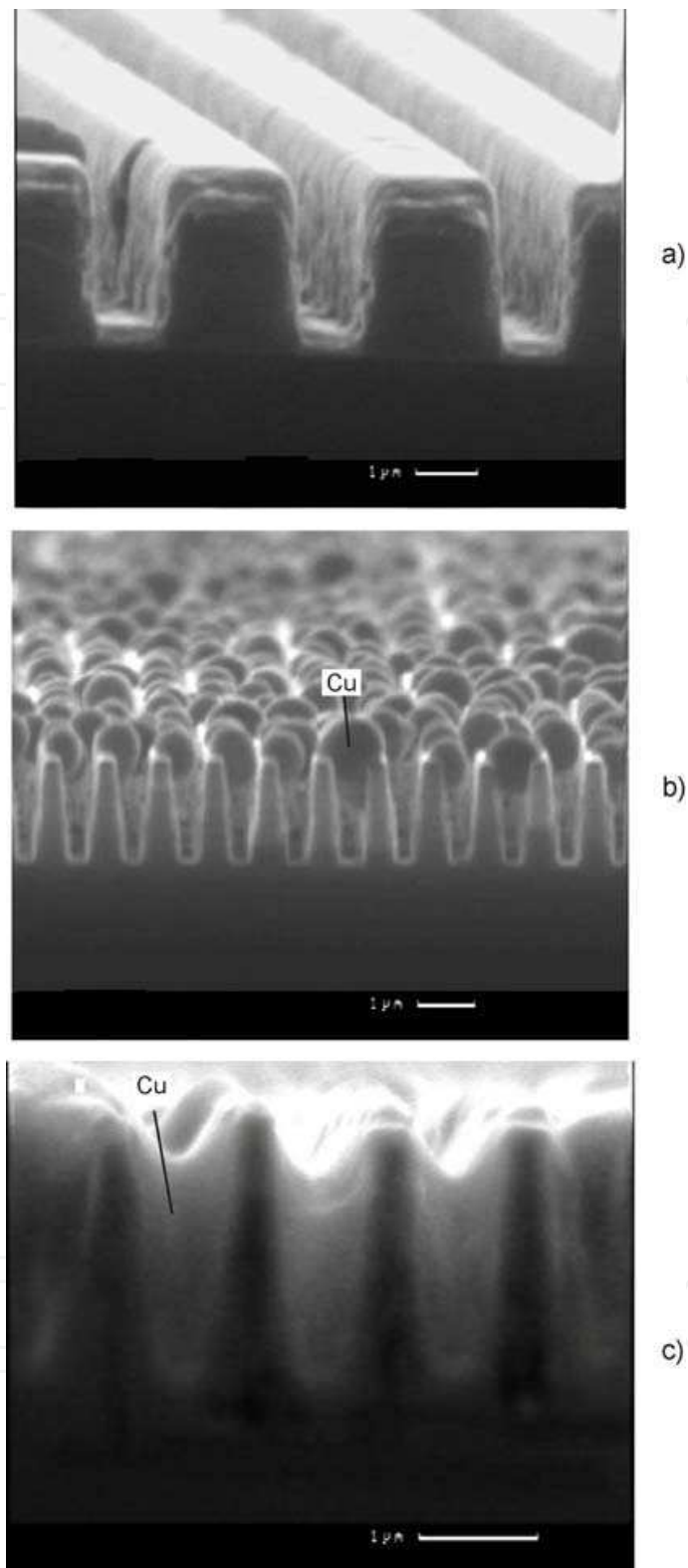


Fig. 17. Heterogeneous melting of the copper thin film deposited on the structure with trenches in SiO_2 coated by the layer of the amorphous Ta-W-N alloy: (a) dispersion into droplets as a result of heat treatment at 1123 K and (b) flow in the trenches as a result of heat treatment at 1123 K owing to the introduction of the wetting 20 nm thick titanium layer between the Ta-W-N layer and the copper film.

The Al-Si system has a phase diagram of the eutectic type. Aluminum almost does not dissolve in Si, while up to 1.65 at % Si can dissolve in aluminum. The eutectic melts at a temperature of 577°C. A result of such character of the interaction in the system is the dissolution of silicon from the substrate in aluminum at relatively low temperatures; i.e., aluminum acts as a solvent of silicon.

It was experimentally established that the appearance of punctures of *p-n* junctions is associated with the above vacancy holes formed as a result of inhomogeneous dissolution of silicon in aluminum (Fig18). The holes are filled with aluminum, which contains dissolved silicon and can cause the shorting of *p-n* junctions. The depth of penetration of aluminum into silicon estimated from the hole depth in local regions near the contact is almost unchanged in the range 300–500°C and is 40–90 nm. In the temperature range 500–577°C, the penetration depth sharply increases to 1.25–1.45 μm.

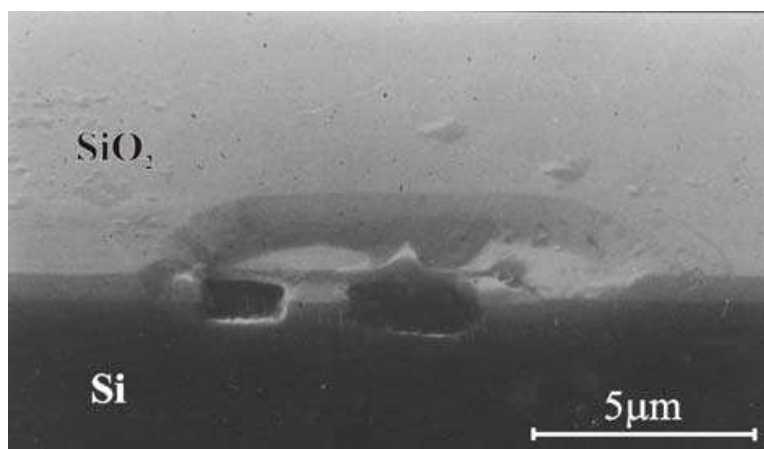
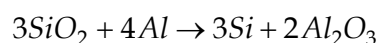


Fig. 18. SEM micrography of the surface morphology of the contact window after heat treatment at 470 °C for 30 minutes and remove the aluminum film.

There was no question that this inhomogeneous dissolution of silicon, filling of the formed holes with aluminum, and the above sharp increase in the penetration depth of aluminum into silicon in the range 500–577°C are due to the appearance of the liquid phase that “melts” silicon, although the heat treatment temperature is lower than the eutectic melting temperature. This circumstance is also confirmed by the fact that the amount of silicon dissolved in aluminum significantly exceeds the amount that should dissolve in aluminum according to the phase diagram at the aforementioned temperature of heat treatment.

It was believed that the reason for the appearance of the liquid phase at a lowered temperature can be local sites with a temperature above 577°C, which can be formed as a result of a strong exothermic reaction between aluminum and the residual natural silicon oxide



which results in an energy released of 220 kJ per mole of the reacting oxide. However, the natural oxide is removed before the deposition of the aluminum film. Although the quasi-oxide SiO_x can remain on the silicon surface, its thickness is ~0.4–0.5 nm (i.e., 1–2 monolayers), which is unlikely sufficient to heat the film to the eutectic melting temperature due to the heat released as a result of the quasi-oxide reduction.

Moreover, the occurrence of meltings was detected at a lower temperature. Heat treatment of integral circuits structures having contact to the silicon layer of titanium, two levels of current-carrying interconnects Al-Si (1%)-Ti (0.5%), separated by a dielectric layer, and

diffusion-barrier layer of TiN, separating the contact layer of titanium and the first level of current-carrying interconnects, at 450 °C resulted in the formation of voids filled with aluminum in silicon, as can be seen in Fig. 19. Analysis of the distribution share of degraded contacts area of the plates showed that this distribution is uneven and random. It should be noted that most nucleation of voids starts at the edges of contact windows (Fig. 19).

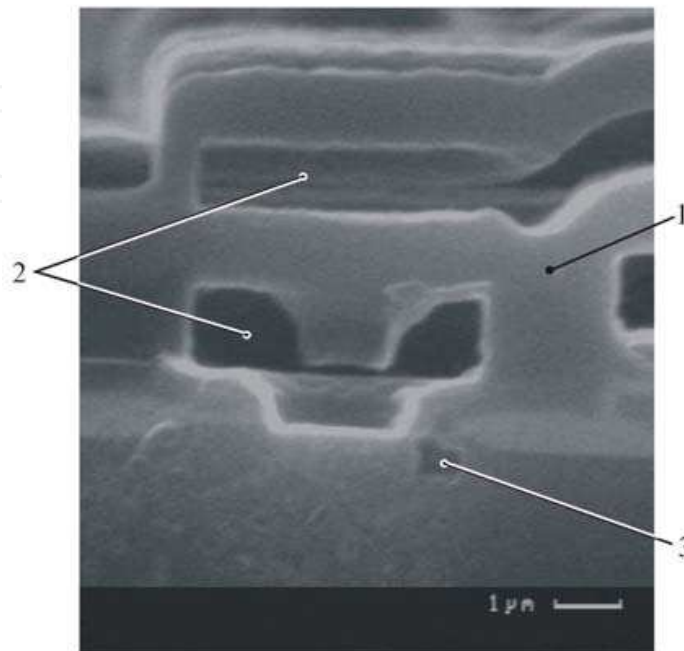


Fig. 19. SEM micrography of the integrated circuit structure cross-section with a two-level metallization after heat treatment at 450 °C for 30 min, and the selective removal of Al: 1 - interlevel SiO₂; 2 - the aluminum interconnects, 3 - penetration of aluminum into silicon in the contact window area.

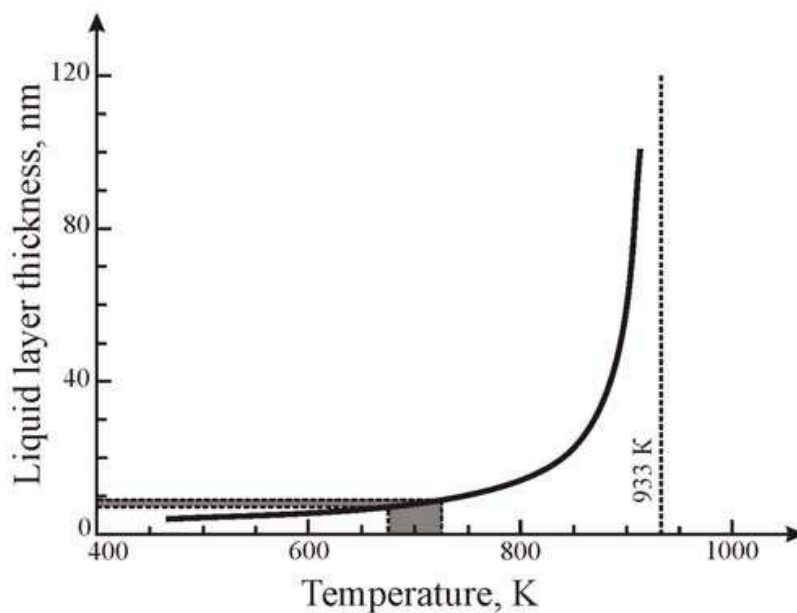


Fig. 20. Temperature dependence of liquid layer thickness on the surface of aluminium, calculated using relationship (10).

For the liquid phase to appear, the formation of the local sites with a temperature higher than the eutectic temperature is not necessary. The formation of such local sites is reasonably explained from the standpoint of the heterogeneous melting under consideration. The calculations (Fig. 20) performed using relationship show that even at temperatures of 400–450°C, which are substantially lower than the eutectic temperature (577°C), a 8–10 nm thick liquid layer should exist on the aluminum surface.

4.4 layer-by-layer growth of crystals and epitaxy

In our opinion, the phenomenon of the heterogeneous melting allows one to understand the vapor–liquid–solid mechanism of epitaxy, which occurs at a temperature below the reference melting temperature, and the mechanism of layer-by-layer growth of crystals.

The mechanism of layer-by-layer growth is observed in the growth from gaseous phase, melts, and solutions. Crystals frequently grow by the crystallization immediately of polymolecular layers, whose thickness is 10–1000 nm, rather than by monomolecular layers as follows from the Gibbs–Kossel–Stranski model. The essence of this mechanism is as follows. Near the crystal surface, there arises a layer that has a polymolecular thickness and completely consists of the crystal-forming material supersaturated with respect to the surrounding mother medium. The layer almost instantaneously crystallizes on a crystal face as a whole plate. The release of the heat of crystallization produces the crystallization pressure, which, in turn, causes outflow of the crystal-forming material from the newly formed crystal surface. Thereafter, the process of formation of the supersaturated polymolecular layer again starts near the crystal surface. Thus, the crystal growth takes a periodicity and becomes pulsating owing to the existence of the incubation period, which is necessary for the formation of each new layer. This layer, which they called the transition layer, “represents as if an independent second medium, micromedium, thinnest shell surrounding the growing crystal. In the medium, a new force field acts and the distribution of particles follows the laws of this field, namely, the potential field of forces.”

However, a substantial gap in this mechanism is a total absence of a clarity regarding the reasons for the appearance of the layer near the crystal surface and its crystallization at some thickness.



Fig. 21. Layer-by-layer grown crystal.

This gap can be filled by the approach based on the mechanism of heterogeneous melting. Recall that the heterogeneous melting is the equilibrium coexistence of a liquid layer with some thickness quite specific at a given temperature and the bulk crystalline phase, e.g., a

crystal. In our opinion, the layer of the liquid phase on the crystal surface formed as a result of the heterogeneous melting is the transition layer proposed above. Thus, it is more correct to consider that this is not a layer near the crystal surface but it is a layer on the crystal surface, which certainly exhibits a particular ordering dictated by the crystalline phase.

Taking into account the heterogeneous melting, the mechanism of layer-by-layer growth should be complemented as follows. At the initial instant of time, at a temperature of the crystal growth, owing to the heterogeneous melting phenomenon, there exists (on the crystal surface) a fairly ordered layer of the own liquid phase with an equilibrium thickness, whose atoms occupy positions dictated by the potential field of the crystal (Fig.22(a)).

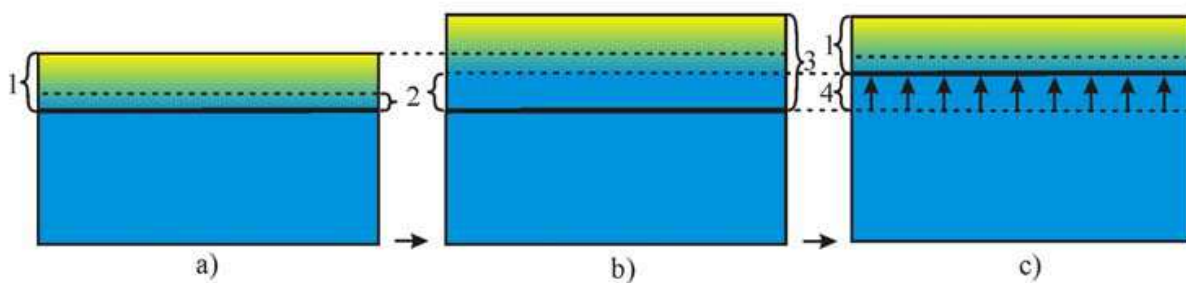


Fig. 22. Schematic diagram of layer-by-layer growth of crystals and epitaxy: 1 – liquid layer with an equilibrium thickness; 2 – ordered part of the liquid layer; 3 – increase of liquid layer thickness beyond equilibrium one; 4 – crystallized layer.

Under conditions of overcooling or supersaturation, under which the crystal grows, a new material continuously transfers to the liquid phase from the mother phase (gaseous phase, melt, or solution that differ from the liquid phase on the crystal surface in the composition, degree of ordering, or concentration) and is continuously ordered inside this liquid phase according to the distribution of the potential field of the crystal. As a result, the thickness of the liquid layer on the crystal surface increases and becomes larger than the equilibrium thickness (Fig. 22 (b)).

The disturbance of the equilibrium state leads to the fact that the layer cannot exist at the given temperature, which inevitably causes the crystallization and a decrease in the thickness of the liquid layer to an equilibrium value (the degree of excess of this thickness over the equilibrium value is determined by the work on displacing the interface between the liquid and crystalline phases) (Fig. 22 (c)). An important peculiarity of the layer-by-layer growth mechanism is that, even if the released heat of crystallization does not displace the liquid-phase atoms (which has not had time to occupy ordered positions) to the mother phase, this heat is responsible for the strong disordering of the remaining liquid-phase layer, so that, at this instant of time, the liquid – crystal interface appears to most abrupt.

Then, the incubation period of ordering of the liquid phase under the action of the potential field of the crystal starts again with a continuous increase in its thickness due to the transfer of the material from the mother phase.

In our opinion, this mechanism of layer-by-layer growth also takes place in the epitaxy, in particular, the vapor-phase epitaxy, which proceeds by so-called vapor – liquid – solid mechanism.

For example, in the chloride method of silicon vapor-phase homoepitaxy, the temperature at which a perfect epitaxial layer grows is 1250°C (the so-called diffusion region where the limiting stage of the process is the transfer of reagents to the solid-phase surface), which is

almost 200°C lower than the reference melting temperature of silicon. In this case, the liquid layer was experimentally observed on the silicon substrate surface. The calculations performed using relationship (10) show (Fig. 23) that the heterogeneous melting should really cause, at a temperature of 1250 °C, the appearance of the 4-nm-thick liquid layer on the surface. However, at a temperature of 900°C, which corresponds to the kinetic region, where the limiting stage of the process is considered to be the chemical reaction itself, the equilibrium thickness of the liquid layer according to the calculations should be only 0.5-1.0 nm (i.e., 2-3 mono-atomic layers). This corresponds to the vapor-solid mechanism observed for the kinetic region.

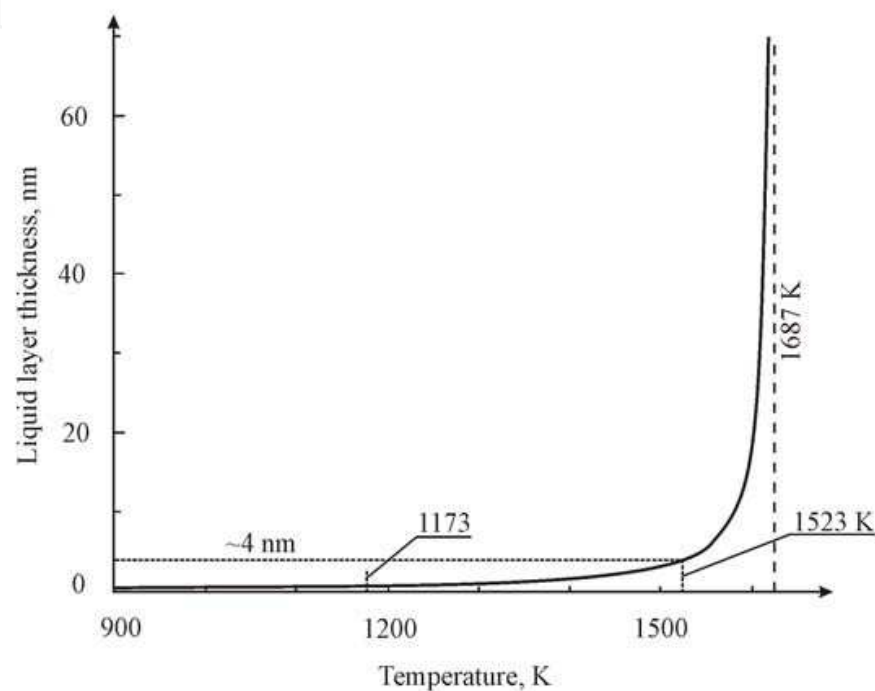


Fig. 23. Temperature dependence of liquid layer thickness on the surface of silicon, calculated using relationship (10).

Taking into account heterogeneous melting the mechanism of layer-by-layer growth allows one to understand how it is possible to decrease the temperature of the silicon homoepitaxy process, which is necessary to suppress the process of autodoping without substantial damage to the epitaxial layer quality. On the one hand, a decrease in the temperature of the process leads to a decrease in the equilibrium thickness of the liquid layer and, on the other hand, to an increase in the viscosity of the liquid and, hence, to a longer ordering of the atoms in the liquid layer. In this connection, the vapor-gas mixture should be added portion-wise. The time interval between the portions is determined by three subsequent stages: 1st stage - ordering of the liquid layer atoms, 2d stage - a decrease in the process temperature in order to induce the crystallization of the ordered liquid layer; and 3d stage - the return of the temperature to the previous level.

4.5 Growth of carbon nanotubes

Growth of carbon nanotubes is also based on the mechanism similar to the mechanism of layer-by-layer crystal growth with the participation of the liquid phase formed as a result of the heterogeneous melting at a temperature lower than the reference melting temperature.

A necessary participant of the process is a set of metal-catalyst droplets. Among such metals are Fe, Co, Ni, Pd, and others, which at high metal concentration have a phase equilibrium diagram with carbon, shown in Fig. 24 for the nickel-carbon system as an example. A specific feature of the diagram is a higher solubility of carbon in liquid nickel as compared to solid nickel.

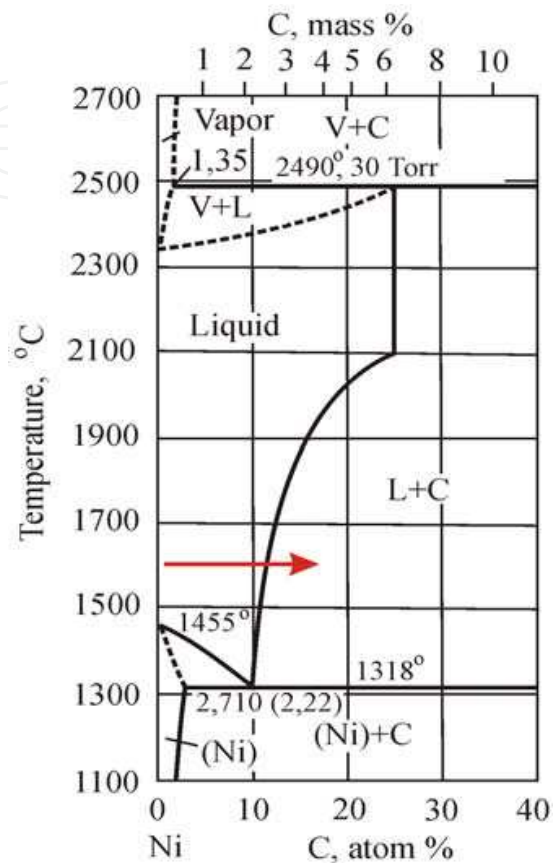


Fig. 24. Phase diagram of the nickel-carbon system.

As stated above, as the thin-film thickness decreases, the phase equilibrium between the liquid and solid phases for the film is shifted towards lower temperatures. For example, for the 50-nm-thick nickel film, this leads to the dispersion of the film into droplets with the participation of the liquid phase at a temperature that is 700° C lower than the reference melting temperature of nickel. Moreover, it was shown that a decrease in the sizes is accompanied by changing all the other equilibrium curves, so that the entire phase diagram is modified and shifted toward lower temperatures.

As a result, the mechanism of growth of carbon nanotubes occurs as follows. At a growth temperature (600–800°C), a nickel droplet 10–50 nm in size represents a crystalline core surrounded by a liquid shell, with an equilibrium thickness, formed due to the heterogeneous melting (Fig. 25 (a)).

When the vapor-gas mixture is fed to the liquid shell surface, there arises a catalytic reaction of decomposition of a carbon-containing organic compound with dissolution of carbon in the nickel liquid phase. A saturation of the nickel liquid layer with carbon increases its thickness and decreases the surface curvature. This disturbs the system from equilibrium (Fig. 25 (b)): as the liquid-layer thickness increases, the lines of equilibrium between the liquid layer and the crystalline core shift towards higher temperatures (see relationship (10)).

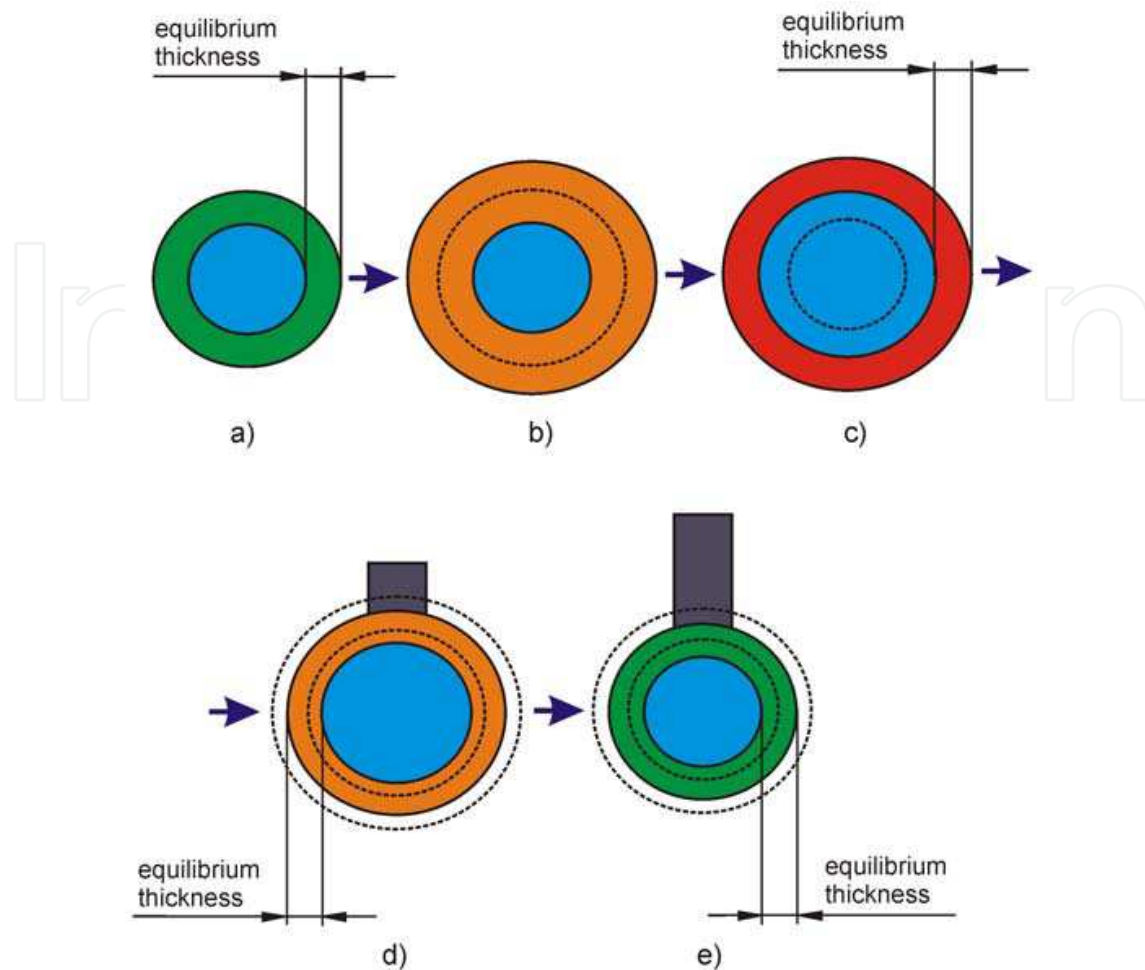


Fig. 25. Scheme of carbon nano-tubes growth.

This results in the initiation of the crystallization, which increases the volume of the crystalline core of the nickel droplet at the expense of nickel from the liquid shell and as a consequence, decreases the volume of the liquid shell (Fig. 25 (c)). In this case, since the solubility of carbon in the nickel liquid phase is much higher than that in the solid phase, carbon remains in the liquid phase and its concentration in the phase sharply increases. Eventually, this results in a supersaturation of the liquid with carbon and the transition to the two-phase region L+C of the coexistence of crystalline carbon and liquid; i.e., carbon precipitates as an individual crystalline phase in the form of nanotubes (Fig. 25(d)).

The released heat of crystallization leads to a partial melting of the crystalline core of the nickel droplet and the system reverts to its original state (Fig. 25(e)). Then, the entire process is repeated. Thus, the process of growth of carbon nanotubes is also periodic and pulsating.

5. Conclusions

Melting of real objects is always a process of heterogeneous melting, since the real objects always possess a surface. It follows from the classical thermodynamics that a liquid layer appears on a solid-phase surface at temperatures that are lower than the reference equilibrium melting temperature of the bulk material. Depending on temperature, certain thickness of the liquid layer on the surface is in equilibrium with the other crystalline phase.

Complete melting of a semi-infinite system occurs near the reference equilibrium melting temperature and does not need a substantial superheating.

The phenomenon of heterogeneous melting is particularly marked in low-dimensional systems, when an equilibrium thickness of the liquid layer becomes comparable to the sizes of objects. In this case, as the sizes decrease, the equilibrium melting temperature significantly decreases to the level lower than the reference temperature.

The process of heterogeneous melting initiates a number of other processes and mechanisms, such as the dispersion of a thin film into droplets, filling of narrow holes with a material of the conformally deposited thin film, the mechanism of vapor-liquid-solid epitaxy, the mechanism of layer-by-layer crystal growth, and the mechanism of growth of carbon nanotubes.

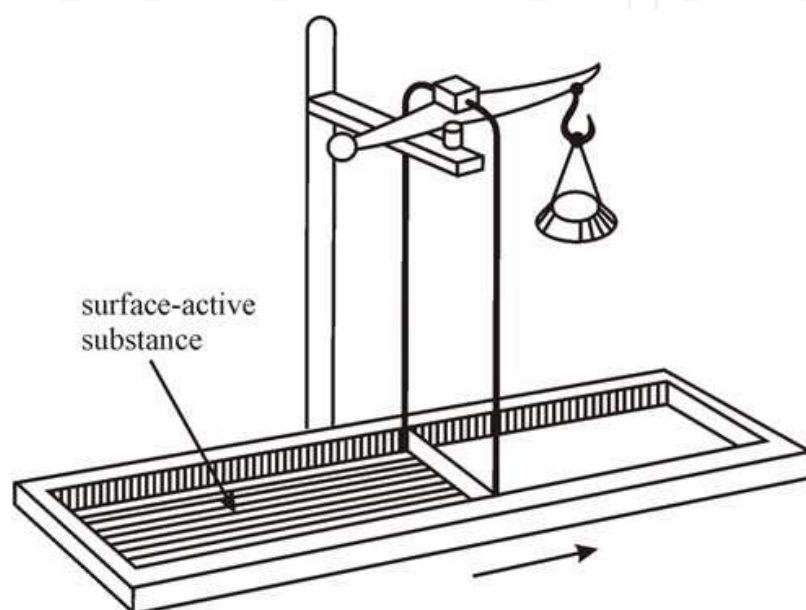


Fig. 26. Langmuir-Adam's Scales scheme.

Understanding of the heterogeneous nature of melting, perhaps, allows us to take another look at the processes of surface and grain boundary diffusion. Scales of Langmuir-Adams, which are designed to measure the surface tension forces, can exemplify this (fig.26). Scales are the movable frame, which touches the surface of the liquid and can easily move. If we add a surfactant (a surface active substance) onto one side of the frame, the frame will move in the direction indicated by the arrow. This process can be considered as a proof that the surface tension force does work on the movement of the frame, applying more energy surface on the other side of the frame. But at the same time, this process can turn out to be a rapid spread of a surface active substance on the surface (which determines the frame speed limit) i.e. the process of surface diffusion. Thus, taking into consideration both processes leads us to the conclusion that high surface diffusion coefficients can be explained by the work done by the surface tension force.

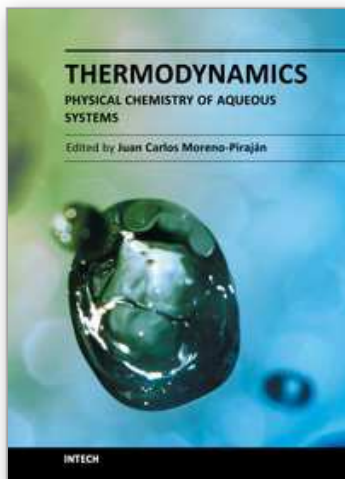
Probably heterogeneous melting process also affects the process of interaction of metal layers with the silicon substrate, which, while observing, first demonstrates the formation of an amorphous (i.e. liquid-like) layer at the interface metal-silicon, and only after that the formation of crystalline silicide compounds.

Diversity of phenomena, which can be explained by the heterogeneous melting participating in them, in our opinion, indicates the reliability of the approach proposed in this work.

6. References

- Andrievskii R. A. & Ragulya A. V. (2005) *Nanostructured Materials*, Akademiya, Moscow, [in Russian]
- Belousov, S. S., Gavrilov, S. A., Gromov, D. G., Redichev, E. N. & Chulkov I. S. (2007). Investigation and Modeling of Low-Dimensional System Melting Temperature. *Izv. Vyssh. Uchebn. Zaved., Elektron.*, No. 1, pp. 15-21, ISSN 1561-5405 [in Russian]
- Buffat, Ph. & Borel, J.-P. (1976). Size effect on the melting temperature of gold particles. *Physical Review A*, Vol. 13, No 6, pp. 2287-2298, ISSN 1050-2947
- Buzdugan, A. A., Gavrilov, S. A., Gromov, D. G., Redichev, E. N. and Chulkov, I. S. (2008). Phenomenological Description of Dispersion of 8–60-nm-Thick Silicon Thin Films into Drops on Al₂O₃ Inert Surface. *Semiconductors*, Vol. 42, No. 13, pp. 1487–1491, ISSN 1063-7826
- Cahn, J. W. (1977). Critical Point Wetting. *Journal of Chemical Physics*, Vol. 66, p. 3667-3772, ISSN 0021-9606
- Cahn, J. W. (1982). Transitions and Phase Equilibria Among Grain Boundary Structures. *Proceedings of Conference on the Structure of Grain Boundaries, Caen, France. Journal de Physique*, Vol. 43, pp. C6 199-213, ISSN 0449-1947
- Chernov, A. A. & Mikheev, L. V. (1988). Wetting of Solid Surfaces by a Structured Simple Liquid: Effects of Fluctuations. *Physical Review Letters*, Vol. 60, No 24, p. 2488-2491, ISSN 0031-9007
- Chernov, A. A. & Mikheev, L. V. (1989). Wetting and Surface Melting: Capillary Fluctuations vs. Layerwise Short-Range Order. *Physica A*, Vol. 157, pp. 1042-1058, ISSN 0378-4371
- Chernov, A. A. & Yakovlev, V. A. (1987). Thin Boundary Layers of the Melt of a Biphenyl Single Crystal and Its Premelting. *Langmuir*, Vol. 3, pp. 635-640, ISSN 0743-7463
- Chistyakov, Yu. D. & Rainova, Yu. P. (1979). *Physicochemical Foundations of Microelectronic Technology*. Metallurgiya, Moscow [in Russian].
- Dostanko, A. P. , Baranov, V. V. & Shatalov V. V. 1989. *Current Carrying Film Systems for VLSI Application*, Vysheishaya Shkola, Minsk [in Russian].
- Emsley J. (1991). *The Elements*, Oxford University Press, Oxford
- Geguzin, Ya. E. (1984). *Physics of Sintering*, Nauka, Moscow, [in Russian]
- Goodman, R. M., Farrell, H. H. & Somorjai, G. A. (1968). Mean Displacement of Surface Atoms in Palladium and Lead Single Crystals. *Journal of Chemical Physics*, Vol. 48, pp.1046-1051,
- Gromov, D. G., Gavrilov, S. A. & Redichev, E. N. (2005). Influence of the Thickness of Copper Films in Cu/W-Ta-N, Cu/C, and C/Cu/C Layered Structures on the Temperature of the Melting-Dispersion Process. *Russian Journal of Physical Chemistry*, Vol. 79, No 9, pp.1394-1400, ISSN 0036-0244
- Gromov, D.G. & Gavrilov S.A. (2009). Manifestation of the heterogeneous mechanism upon melting of low-dimensional systems. *Physics of the Solid State*, Vol. 51, No. 10, pp. 2135–2144, ISSN 1063-7834
- Gromov, D.G., Gavrilov, S.A., Redichev, E.N. & Ammosov R.M. (2007). Kinetics of the melting-dispersion process in copper thin films. *Physics of the Solid State*, Vol. 49, No 1, pp.178-184, ISSN 1063-7834
- Gromov, D.G., Gavrilov, S.A., Redichev, E.N., Chulkov, I.S., Anisimov M. Y., Dubkov, S.V. & Chulkov, S.I. (2010). Non-monotonic dependence of temperature of Au nanometer films dissociation into droplets on their thickness on Al₂O₃ surface. *Applied Physics A*, Vol. 99, pp. 67-71, ISSN 0947-8396

- Gromov, D.G., Gavrilov, S.A., Redichev, E.N., Klimovitskaya, A.V. & Ammosov R.M. (2006). The factors that determine the temperature of fusion of Cu and Ni thin films on inert surfaces. *Russian Journal of Physical Chemistry*, Vol. 80, No 10. pp.1650-1655, ISSN 0036-0244
- Gromov, D.G., Mochalov, A.I., Klimovitskiy, A.G., Sulimin, A.D. & Redichev, E.N. (2005). Approaches to diffusion barrier creation and trench filling for copper interconnection formation. *Applied Physics A*, Vol. 81, № 7, pp.1337-1343, ISSN 0947-8396
- Gusev, A. I. & Rempel A. A. (2004). *Nanocrystalline Materials*, Fizmatlit, Moscow, Cambridge International Science, Cambridge
- Gusev, A. I. (2005). *Nanomaterials, Nanostructures, and Nanotechnologies*, Fizmatlit, Moscow, [in Russian]
- Handbook of Physical Quantities*. (1996). I. S. Grigoriev & E. Z. Meilikhov (Eds.), Energoatomizdat, Moscow, CRC Press, Boca-Raton, FL, United States
- Hansen, M. & Anderko, K. (1958). *Constitution of Binary Alloys*, McGraw-Hill Book Company, New York
- Kiselev, V. F., Kozlov, S. N. & Zoteev, A. V. (1999). *Fundamentals of the Solid Surface Physics*, Moscow State University, Moscow [in Russian]
- Komnik, Yu. F. (1979). *Physics of Metal Films: Dimensional and Structural Effects*, Atomizdat, Moscow, [in Russian]
- Müller, P. & Kern R. (2003). Surface melting of nanoscopic epitaxial films. *Surface Science*, Vol. 529, pp. 59-94, ISSN 00396028
- Pluis, B., Denier van der Gon, A. W. and van der Veen J. F. (1990). Surface-induced melting and freezing. I. Medium-energy ion scattering investigation of the melting of Pb{hkl} crystal faces. *Surface Science*, Vol. 239, p.265-281, ISSN 00396028
- Processes of the Real Crystal Formation*. (1977). N. V. Belov (Ed.), Nauka, Moscow [in Russian].
- Redichev, E.N., Gromov, D.G., Gavrilov, S.A., Mochalov, A.I. & Ammosov, R.M. (2006). Combined method of copper electroplating deposition and low temperature melting for damascene technology. *Proceedings of SPIE*, Vol. 6260, SPIE, Bellingham, WA, pp. 62601H1-62601H1.
- Roldugin, V. I. (2008). *Physicochemistry of the Surface*, Intellect, Dolgoprudnyi, Moscow region, Russia, [in Russian]
- Shigeta, Y. & Fukaya, Y. (2004). Structural phase transition and thermal vibration of surface atoms studied by reflection high-energy electron diffraction. *Applied Surface Science*. Vol. 237, p. 21-28, ISSN 0169-4332
- Suzdalev, I. P. (2006). *Nanotechnology: Physical Chemistry of Nanoclusters, Nanostructures, and Nanomaterials*, KomKniga, Moscow, [in Russian]
- Tartaglino, U., Zykova-Timan, T., Ercolessi F. & Tosatti, E. (2005). Melting and nonmelting of solid surfaces and nanosystems. *Physics Reports*, Vol. 411, No 5, pp. 291-321, ISSN 0370-1573.
- Wautelet, M., Dauchot, J. P. & Hecq, M. (2000). Phase diagrams of small particles of binary systems: a theoretical approach. *Nanotechnology*, Vol. 11, pp. 6-9, ISSN: 1550-7033



Thermodynamics - Physical Chemistry of Aqueous Systems

Edited by Dr. Juan Carlos Moreno Piraján

ISBN 978-953-307-979-0

Hard cover, 434 pages

Publisher InTech

Published online 15, September, 2011

Published in print edition September, 2011

Thermodynamics is one of the most exciting branches of physical chemistry which has greatly contributed to the modern science. Being concentrated on a wide range of applications of thermodynamics, this book gathers a series of contributions by the finest scientists in the world, gathered in an orderly manner. It can be used in post-graduate courses for students and as a reference book, as it is written in a language pleasing to the reader. It can also serve as a reference material for researchers to whom the thermodynamics is one of the area of interest.

How to reference

In order to correctly reference this scholarly work, feel free to copy and paste the following:

Dmitry G. Gromov and Sergey A. Gavrilov (2011). Heterogeneous Melting in Low-Dimensional Systems and Accompanying Surface Effects, *Thermodynamics - Physical Chemistry of Aqueous Systems*, Dr. Juan Carlos Moreno Piraján (Ed.), ISBN: 978-953-307-979-0, InTech, Available from:
<http://www.intechopen.com/books/thermodynamics-physical-chemistry-of-aqueous-systems/heterogeneous-melting-in-low-dimensional-systems-and-accompanying-surface-effects>

INTECH

open science | open minds

InTech Europe

University Campus STeP Ri
Slavka Krautzeka 83/A
51000 Rijeka, Croatia
Phone: +385 (51) 770 447
Fax: +385 (51) 686 166
www.intechopen.com

InTech China

Unit 405, Office Block, Hotel Equatorial Shanghai
No.65, Yan An Road (West), Shanghai, 200040, China
中国上海市延安西路65号上海国际贵都大饭店办公楼405单元
Phone: +86-21-62489820
Fax: +86-21-62489821

© 2011 The Author(s). Licensee IntechOpen. This chapter is distributed under the terms of the [Creative Commons Attribution-NonCommercial-ShareAlike-3.0 License](#), which permits use, distribution and reproduction for non-commercial purposes, provided the original is properly cited and derivative works building on this content are distributed under the same license.

IntechOpen

IntechOpen